HHS Public Access

Author manuscript

Mol Microbiol. Author manuscript; available in PMC 2018 May 01.

Published in final edited form as:

Mol Microbiol. 2017 May ; 104(3): 377–399. doi:10.1111/mmi.13632.

Insufficient levels of the *nrdAB*-encoded ribonucleotide reductase underlie the severe growth defect of the Δ*hda E. coli* strain

Vignesh M. P. Babu[1,#], **Mark Itsko**[2], **Jamie C. Baxter**[1,%], **Roel M. Schaaper**[2], and **Mark D. Sutton**[1,*]

[1]Department of Biochemistry, Jacobs School of Medicine and Biomedical Sciences, University at Buffalo, State University of New York, Buffalo, NY, USA

[2]Genome Integrity and Structural Biology Laboratory, National Institute of Environmental Health Sciences, Research Triangle Park, NC, USA

Abstract

The ATP-bound form of the *Escherichia coli* DnaA replication initiator protein remodels the chromosomal origin of replication, *oriC*, to load the replicative helicase. The primary mechanism for regulating the activity of DnaA involves the Hda and β clamp proteins, which act together to dramatically stimulate the intrinsic DNA-dependent ATPase activity of DnaA via a process termed Regulatory Inactivation of DnaA (RIDA). In addition to hyper-initiation, strains lacking *hda* function also exhibit cold sensitive growth at 30°C. Strains impaired for the other regulators of initiation (i.e., Δ*seqA* or Δ*datA*) fail to exhibit cold sensitivity. The goal of this study was to gain insight into why loss of *hda* function impedes growth. We used a genetic approach to isolate 9 suppressors of Δ*hda* cold sensitivity, and characterized the mechanistic basis by which these suppressors alleviated Δ*hda* cold sensitivity. Taken together, our results provide strong support for the view that the fundamental defect associated with Δ*hda* is diminished levels of DNA precursors, particularly dGTP and dATP. We discuss possible mechanisms by which the suppressors identified here may regulate dNTP pool size, as well as similarities in phenotypes between the Δ*hda* strain and *hda*$^+$ strains exposed to the ribonucleotide reductase inhibitor hydroxyurea.

ABBREVIATED SUMMARY

Loss of *E. coli hda* function results in the accumulation of DnaA-ATP, causing hyper-initiation and altered transcription of DnaA-regulated genes, including *nrdAB*, which encode ribonucleotide reductase. We identified 9 suppressors of Δ*hda* that had in common the ability to restore cellular dNTPs to near wild type levels in the absence of *hda* function, suggesting that the significant reduction in *nrdAB* expression observed in the Δ*hda* strain underlies its growth defect.

[*]**Corresponding author:** Department of Biochemistry, Jacobs School of Medicine and Biomedical Sciences, University at Buffalo, State University of New York, 140 Farber Hall, 3435 Main Street, Buffalo, NY, 14214, USA., Phone: (716) 829–3581, Fax: (716) 829-2661, mdsutton@buffalo.edu.
[#]**Current address:** Department of Biology, Massachusetts Institute of Technology, Cambridge, MA, 02139, USA.
[%]**Current address:** Department of Molecular Genetics, University of Toronto, Toronto, Ontario M5S 1A8, Canada.

The authors declare that they have no conflict of interest.

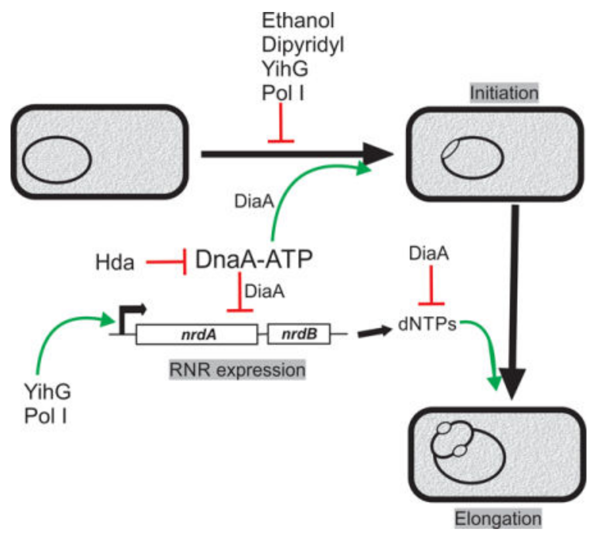

INTRODUCTION

DNA replication in *E. coli* initiates at a single origin, *oriC*, by a mechanism that requires the DnaA protein (Crooke *et al.*, 1993, Margulies & Kaguni, 1996, Kaguni, 2006, Duderstadt *et al.*, 2011, Duderstadt *et al.*, 2010, Leonard & Grimwade, 2010, Chodavarapu & Kaguni, 2016). The ATP-bound form of the DnaA replication initiator protein (DnaA-ATP) is active for initiation of replication. To initiate DNA replication, DnaA-ATP must cooperatively bind several DnaA-boxes within *oriC* (Margulies & Kaguni, 1996, Leonard & Grimwade, 2011). Binding to these sites mediates opening of the AT-rich DNA unwinding element and subsequent loading of the DnaB helicase onto the unwound single strand (ss) DNA (Carr & Kaguni, 2001, Sutton *et al.*, 1998, Marszalek & Kaguni, 1994, Seitz *et al.*, 2000). The timing of this process is highly regulated to ensure proper coordination with the cell cycle (Katayama *et al.*, 2010, Kawakami & Katayama, 2010). There are at least 3 distinct mechanisms that regulate the timing of replication initiation (reviewed in (Katayama *et al.*, 2010)). One involves sequestration of newly replicated *oriC* away from DnaA-ATP by the SeqA protein (Lu *et al.*, 1994, Slater *et al.*, 1995, Wold *et al.*, 1998, Nievera *et al.*, 2006), while the other two utilize *datA* and *hda*, respectively, to dramatically stimulate the intrinsic DNA-dependent ATPase activity of DnaA, leading to formation of DnaA-ADP that is inactive in initiation due to its non-specific DNA binding activity. Although both *datA* and *hda* stimulate conversion of DnaA-ATP to DnaA-ADP, they utilize distinct mechanisms. Binding of DnaA-ATP to the *datA* locus results in a nucleoprotein complex with enhanced ATPase activity compared to other DnaA-box containing sequences (Kasho & Katayama, 2013). This process is termed *datA*-dependent DnaA-ATP Hydrolysis, or DDAH. The *datA* locus may additionally act as a 'sink' for DnaA-ATP, sequestering a subpopulation of DnaA-ATP away from *oriC* (Kitagawa *et al.*, 1996). In contrast to *datA*, Hda, in complex with the *dnaN*-encoded β sliding clamp protein assembled on double strand (ds) DNA, interacts with DnaA-ATP to stimulate its ATPase activity via a process termed Regulatory Inactivation of DnaA, or RIDA (Katayama *et al.*, 1998, Kato & Katayama, 2001, Su'etsugu *et al.*, 2005). RIDA is thought to occur during replication, either at the replication fork, or on clamps left behind on lagging strand (Collier & Shapiro, 2009, Fernandez-Fernandez *et al.*, 2013, Su'etsugu *et al.*, 2004). Whereas DDAH is estimated to account for hydrolysis of ~20% of the DnaA-ATP, RIDA accounts for the rest (Kasho & Katayama, 2013).

Consistent with its established role in regulating the ratio of DnaA-ATP/DnaA-ADP, loss of *hda* function leads to hyper-initiation of DNA replication and genome instability (Kato & Katayama, 2001, Charbon *et al.*, 2014, Simmons *et al.*, 2004). The Δ*hda* allele also confers slow growth at 37°C (Riber *et al.*, 2006), as well as a severe cold sensitive growth phenotype at 30°C (Baxter & Sutton, 2012). Remarkably, cold sensitive growth is rapidly suppressed following one or two passages at 37°C via an unknown mechanism (Baxter & Sutton, 2012). These phenotypes are not observed with Δ*seqA* or Δ*datA* strains, which also hyper-initiate suggesting Hda may have one or more cellular roles in addition to RIDA. Consistent with this conclusion, Hda may help regulate access of translesion DNA synthesis (TLS) DNA polymerases (Pols) to the replication fork (Baxter & Sutton, 2012).

In addition to its role in initiation, DnaA also influences transcription of several genes, including *nrdAB*, *rpoH*, *guaA*, *polA*, and *dnaA* itself (Quinones *et al.*, 1997, Messer & Weigel, 1997, Kucherer *et al.*, 1986, Braun *et al.*, 1985, Wang & Kaguni, 1987, Wang & Kaguni, 1989). Using *lacZ-nrdA* promoter fusions, the Fuchs lab concluded that DnaA activated transcription of *nrdAB*, which encodes the *E. coli* class 1a ribonucleotide reductase (RNR) (Jacobson & Fuchs, 1998, Augustin *et al.*, 1994). In contrast, based on their analysis of DnaA mutants that either failed to bind ATP or, compared to wild type DnaA had an enhanced intrinsic ATPase activity, the Beckwith lab concluded that DnaA-ATP repressed *nrdAB* transcription by competing with RNA polymerase (RNAP) for binding to the *nrdA* promoter (Gon *et al.*, 2006). Consistent with both of these conclusions, recent work from the Sclavi lab supports both activator and repressor functions of DnaA-ATP at the *nrdA* promoter (Olliver *et al.*, 2010). Activation of *nrdAB* transcription was observed at low concentrations of DnaA-ATP, which failed to block RNAP, while repression was observed at high DnaA-ATP levels capable of forming a nucleoprotein filament that precluded RNAP binding.

At least 4 distinct groups of suppressors have been described that improve growth of the Δ*hda* strain at 37°C. The first group includes alleles that reduce the frequency of hyper-initiation to compensate for the loss of RIDA resulting from Δ*hda*. This group includes, for example, mutations that enhance the intrinsic ATPase activity of DnaA independently of *datA* or *hda* function, or that increase steady state levels of SeqA (Ortenberg *et al.*, 2004, Feeney *et al.*, 2012, Charbon *et al.*, 2011). A second way to suppress the poor growth of the Δ*hda* strain at 37°C is to overproduce RNR (Fujimitsu *et al.*, 2008, Gon *et al.*, 2006). Overexpression of NrdAB also suppressed the growth defect of the *hda-185* (K170C) allele, which is functional at 37°C, but exhibits a Δ*hda* phenotype at 25°C (Fujimitsu *et al.*, 2008). The third group of suppressors include those that limit the generation of 8-oxo-7,8-dihydro-2′-deoxyguanosine (8-oxo-dG), which is a byproduct of aerobic growth, or prevent its excision from nascent DNA leading to single strand (ss) DNA breaks. The Δ*hda* strain suffers dsDNA breaks resulting in large part from the replication fork encountering ssDNA breaks catalyzed by the bifunctional MutM glycosylase/lyase during excision of 8-oxo-dG (Charbon *et al.*, 2014). It is unclear whether the Δ*hda* strain incorporates more 8-oxo-dG than the isogenic *hda*$^+$ strain, making it more likely that forks will encounter ssDNA gaps resulting from 8-oxo-dG repair intermediates, or whether it incorporates comparable levels to wild type but excision of 8-oxo-dG and repair of the ensuing ssDNA gap requires more time than is available before subsequent replication forks encounter them in the hyper-initiating Δ*hda* strain. In addition to these three groups, a fourth group of Δ*hda* suppressors have been described, but their possible mechanism(s) of suppression are unknown (Charbon *et al.*, 2011). Given this range in Δ*hda* suppressors, it is unclear whether suppression addresses a common problem caused by the Δ*hda* allele, or whether there are multiple distinct mechanisms for coping with the Δ*hda* allele. Furthermore, the mechanistic relationship between poor growth of the Δ*hda* strain at 37°C and its failure to grow at 30°C has not been explored.

The goal of this study was to gain insight into why loss of *hda* function impedes growth. To this end, we isolated a total of 9 suppressors of Δ*hda* cold sensitivity, and characterized their abilities, as well as several previously identified suppressors of the 37°C Δ*hda* growth defect to alleviate cold sensitive growth. Based on genomic sequence, the suppressors mapped to 4 distinct loci, including *diaA*, *trmA*, upstream of *nrdA*, and duplication of a 180-kb region between the *rrsA* and *rrsE* genes. With the exception of *trmA*, which was identified in a strain that also contained the 180-kb duplication and was not examined further in this work, each of the other suppressors acted to increase *nrdAB* transcription, effectively increasing the size of the intracellular dNTP pool. Taken together, our results provide strong support for the view that the fundamental defect associated with Δ*hda* is diminished levels of dNTP precursors, particularly dGTP and dATP. We discuss possible mechanisms by which the suppressors identified here may regulate *nrdAB* expression, as well as similarities in phenotypes between the Δ*hda* strain and *hda*$^+$ strains treated with HU.

RESULTS

Identification of suppressors of Δ*hda* cold sensitivity

E. coli strains bearing the Δ*hda* allele grow more slowly at 37°C compared to the isogenic *hda*$^+$ strain (Riber *et al.*, 2006) and are severely impaired for growth at 30°C (Fig. 1A), a phenotype we have termed cold sensitive growth (Baxter & Sutton, 2012). These phenotypes were not observed for Δ*seqA* or Δ*datA* strains (Baxter & Sutton, 2012), suggesting that Hda may have one or more cellular roles in addition to regulating initiation of DNA replication. To gain insight into why loss of *hda* function impaired growth, we screened for Δ*hda* suppressors that permitted growth at 30°C. Briefly, the Δ*hda*::*cat* allele (located at 56.40 min) was transduced from a strain bearing an unlinked suppressor ((Charbon *et al.*, 2011); *hsm*-1, mapping to *seqA* at 15.3 min) into MG1655 at 37°C, resulting in strain JCB100 (MG1655 Δ*hda*::*cat*). Transductants were passaged on LB agar plates at 37°C, then screened for growth at 30°, 37° and 42°C. We identified 9 clones with the ability to grow at 30°C, due to suppressors (named JCB100s1-12, for suppressed), which we designated '*sch*' for suppressors of cold sensitive Δ*hda*, as well as two that lacked this ability (named JCB100u1-2, for unsuppressed) (Fig. 1A). Except for JCB100s10 and JCB100s12, growth of each of the *sch* strains at 30°C was comparable to that of the wild type control. Although, the JCB100s12 strain, and to a lesser extent JCB100s10, exhibited less robust growth at 30°

compared to 37°C, indicating incomplete suppression, they nevertheless grew significantly better than the unsuppressed Δ*hda* strains at 30°C (Fig. 1A).

Since loss of *hda* function leads to hyper-initiation of replication (Kato & Katayama, 2001), we asked whether any of the *sch* alleles decreased the frequency of hyper-initiation caused by Δ*hda* by measuring the copy number of *oriC* relative to *terC* using qPCR. High *oriC/terC* ratios (i.e., ~10) were observed for unsuppressed Δ*hda* strains JCB100u1 and JCB100u2, indicating hyper-initiation (Fig. 1B). In contrast, all 9 JCB100s clones exhibited near wild type *oriC/terC* ratios (i.e., ~3–4). Taken together, these results suggest that the 9 *sch* alleles suppress both cold sensitive growth and hyper-initiation caused by Δ*hda*.

Nucleotide sequence of the *sch* alleles

In order to identify the genetic alteration(s) responsible for each *sch* allele, we isolated genomic DNA from each of the 9 JCB100s strains, as well as the MG1655 parent and sequenced them using the Illumina platform. Eight of the 9 JCB100s strains contained a single alteration relative to our MG1655 reference, while one contained two alterations (Table 1). These mutations clustered to 4 distinct loci: (i) an IS5 inserted within *diaA* (*diaA*::IS5; located at 71.01 min); (ii) IS1 or IS5 insertions upstream of *nrdAB* (50.52 min) (Fig. S1); (iii) a 180-kb duplication of the region between *rrsA* (86.94 min) and *rrsE* (90.66); and (iv) in one of the strains bearing the 180-kb duplication (JCB100s10), a single G-to-A point mutation resulting in a deduced A48T amino acid substitution at position 142 of *trmA* (89.67 min), which encodes a tRNA methyltransferase (Urbonavicius *et al*., 2007). The *trmA* gene is present within the 180-kb duplication and both copies of *trmA* in JCB100s1 carried the A48T mutation. The more robust growth at 30°C of strain JCB100s10 compared to JCB100s12 indicates that the *trmA-A48T* mutation contributes to suppression of Δ*hda* cold sensitivity (Fig. 1A).

Loss of *diaA* function suppresses Δ*hda* cold sensitivity

The *diaA* allele was identified as a loss-of-function suppressor of the cold sensitive (30°C) growth phenotype conferred by the hyperactive *dnaAcos* allele (Ishida *et al*., 2004), and was subsequently determined to also suppress the 25°C growth defect of the *hda-185* allele (Fujimitsu *et al*., 2008). We hypothesized that the *diaA*::IS5 mutation in JCB100s2 was a loss-of-function allele. Therefore, using a previously described quantitative transduction assay (Baxter & Sutton, 2012), we asked whether the Δ*diaA762*::*kan* allele (see Table S2) suppressed Δ*hda* cold sensitivity. Briefly, the Δ*hda*::*cat* allele was transduced into isogenic *diaA*$^+$ (VB001) and Δ*diaA* (VB002) strains, and Cam^R transductants were selected in parallel at both 30° and 42°C. As summarized in Fig. 2A, the Δ*diaA* strain was efficiently transduced to Cam^R at both 30° and 42°C while the *diaA*$^+$ strain could be transduced with Δ*hda* only at 42°C, confirming the ability of Δ*diaA* to suppress Δ*hda* cold sensitivity. We also used qPCR to measure *oriC/terC* ratios in these strains. Consistent with its role in promoting initiation, the Δ*diaA* strain displayed a slightly reduced *oriC* copy number relative to the *diaA*$^+$ control (Fig. 2C). Similar to the phenotype of JCB100s2 (*diaA*::IS5; Fig. 1B), *oriC* copy number in the Δ*diaA* Δ*hda* mutant was reduced to near wild type levels (Fig. 2C). Since a reduced *oriC/terC* ratio could result from either fewer initiation events or more efficient elongation resulting in more forks reaching the terminus, we used flow cytometry to measure genome copies following replication run-out as described previously (Baxter & Sutton, 2012). As summarized in Fig. 3A, loss of *diaA* function reduced genome content, as evidenced by the increased in 2n and reduction in 4n compared to MG1655, indicating it reduced the frequency of initiation. While the Δ*diaA* Δ*hda* strain possessed an elevated number of genomes compared to MG1655, the genome number was nevertheless reduced compared to the unsuppressed Δ*hda* strain (JCB100u1). Thus, loss of *diaA* function both reduced the frequency of initiation and promotes more efficient elongation of replication forks to the terminus in the absence of *hda* function. Finally, the Δ*diaA* allele only partially suppressed the slow growth phenotype of the Δ*hda* strain observed at 37°C (Fig. S2C), suggesting this growth defect was attributable to more than merely hyper-initiation.

Overexpression of RNR suppresses Δ*hda* cold sensitivity

The presence of IS elements upstream of *nrdA* was demonstrated to increase the level of *nrdAB* transcription (Feeney *et al*., 2012), suggesting that *sch-1*, *sch-4*, *sch-6*, *sch-7*, *sch-8* and *sch-9* might suppress Δ*hda* by increasing expression of *nrdAB*. Consistent with this interpretation, as well as previous results, overexpression of *nrdAB* suppressed the growth defect at 37°C of the Δ*hda* strain (Fujimitsu *et al*., 2008, Gon *et al*., 2006), while overexpression of either *nrdAB* or the class 1b RNR *nrdEF* suppressed the 25°C growth defect of the *hda-185* strain (Fujimitsu *et al*., 2008). In light of these findings, we used our quantitative transduction assay discussed above to determine whether a plasmid directing expression of *E. coli nrdAB* (pTKM226) or the class 1b RNR encoded by *nrdEF* (pTKM221) suppressed Δ*hda* cold sensitivity. As controls, we used plasmid pBR322, as well as pMS100, which expresses an inactive NrdA-C439A subunit together with NrdB. As summarized in Fig. 2A, elevated levels of either *nrdAB* or *nrdEF* suppressed Δ*hda* cold sensitivity. In contrast, neither the empty control plasmid (pBR322), nor elevated levels of *nrdA(C439A)B* suppressed, indicating that suppression required elevated levels of active RNR. Based on *oriC/terC* ratios, overexpression of RNR also suppressed hyper-initiation caused by Δ*hda* (Fig. 2C), consistent with published findings (Fujimitsu *et al*., 2008). As summarized in Fig. 3A, overexpression of NrdAB failed to exert an effect on the genome content of MG1655. The Δ*hda* strain bearing the *nrdAB*-expressing plasmid pTKM226 possessed an elevated number of genomes compared to the wild type MG1655 control (Fig. 3B), indicating that elevated levels of NrdAB suppress Δ*hda* by promoting more efficient elongation of replication forks through to the terminus region. Finally, whereas overexpression of *nrdAB* (pTKM226) or *nrdEF* (pTKM221) slowed growth of the hda^+ strain at 37°C, *nrdAB* significantly improved growth of the Δ*hda* strain, while *nrdEF* did so only partially (Fig. S2E & F). Taken together, these results confirm earlier reports that increased levels of RNR suppress the 37°C growth defect of the Δ*hda* strain, as well as the 25°C growth defect of the *hda-185* strain (Fujimitsu *et al*., 2008, Gon *et al*., 2006), and demonstrate that RNR overexpression also suppresses Δ*hda* cold sensitivity.

Multicopy *yihG* or *polA* suppresses Δ*hda* cold sensitivity

The 180-kb *rrsA*-*rrsE* duplication that we identified by virtue of its ability to partially suppress Δ*hda* cold sensitivity is identical to the duplication described by Charbon and colleagues that suppressed the 37°C Δ*hda* growth defect (Charbon *et al*., 2011). However, the basis by which this 180-kb duplication suppressed the 37°C Δ*hda* growth defect was not described. It is interesting that this duplication failed to completely suppress Δ*hda* cold sensitivity (Fig. 1A), despite its ability to suppress at 37°C (Charbon *et al.*, 2011). We hypothesized that one or more of the 153 genes present within the duplicated region suppressed Δ*hda* cold sensitivity by virtue of a two-fold increase in its gene dosage. We further hypothesized that the gene or genes responsible may be DnaA-regulated. We therefore asked whether any of the 153 genes contained within this 180-kb region resided nearby a DnaA-box. The DnaA-box located between *polA* and *yihG* was reported to activate *polA* transcription as cells approached stationary phase (Quinones *et al.*, 1997). The *polA* gene encodes the DNA repair polymerase, Pol I (Joyce *et al.*, 1982), while *yihG* encodes a predicted inner membrane associated acetyl transferase of unknown function (Granseth *et al.*, 2005, Daley *et al.*, 2005). We therefore used pRM100, a low copy number plasmid that directs expression of DNA polymerase I, as well as the first 196 codons of *yihG* (*yihG'*–*polA*), which comprise the putative acetyl transferase domain and all predicted transmembrane helices. Using the same P1*vir* transduction assay described above, we demonstrated that a strain bearing pRM100 was suppressed for Δ*hda* cold sensitivity. Importantly, a plasmid (pVB002) derived from pRM100 that lacks the coding sequence for both *yihG* and *polA*, but retains the complete intergenic promoter region including the DnaA box, failed to suppress Δ*hda* cold sensitivity (Fig. S3). Thus, suppression was not the result of the plasmid-encoded DnaA box titrating DnaA-ATP away from *oriC*. The Δ*hda* pRM100 strain also exhibited a near-wild type *oriC/terC* ratio (Fig. 2B & C). Based on flow cytometry (Fig. 3A), pRM100 reduced genome content of MG1655, similar to Δ*diaA*, indicating that elevated levels of YihG'/Pol I reduced the frequency of initiation. While the Δ*hda* strain bearing pRM100 possessed an elevated number of genomes compared to MG1655, it was nevertheless reduced compared to the Δ*hda* strain (JCB100u1). In light of the qPCR results (Fig. 2), these findings indicate that elevated levels of Pol I promote more efficient elongation of replication forks through to the terminus region and also modestly reduce initiation frequency. Finally, pRM100 fully suppressed the 37°C growth defect of the Δ*hda* strain (Fig. S2D).

To determine whether *yihG* and/or *polA* are responsible for suppression, we assayed plasmids expressing either *yihG* or *polA* for their respective abilities to suppress Δ*hda* cold sensitivity. Based on our quantitative transduction assay, both the *yihG*- and *polA*-expressing plasmids suppressed Δ*hda* cold sensitivity (Fig. 2B). In contrast to Pol I, overexpression of Pol II, Pol IV or Pol V failed to suppress Δ*hda* (Fig. 2B). While it is possible that one or more additional genes within the 180-kb *rrsA*-*rrsE* duplication also contribute to suppression of Δ*hda* cold sensitivity, our results demonstrate that elevated levels of either *yihG* or *polA* are sufficient. These results, taken together with those discussed above, indicate that Δ*hda* cold sensitivity is suppressed by disruption of *diaA* or overexpression of *nrdAB*, *yihG* or *polA*.

Induction of the heat shock response suppresses Δ*hda* cold sensitivity

Results discussed above suggest a relationship between DnaA-dependent regulation of *polA* and Δ*hda* cold sensitivity. We therefore used RNA-seq to measure the transcriptome of the wild type (VB001), Δ*diaA* (VB002) and Δ*diaA* Δ*hda* (VB003) strains to determine whether expression levels of other DnaA regulated genes were altered by Δ*hda*. Genes with expression profiles altered more than 4-fold relative to the wild type strain are listed in Table S1. Remarkably, none of the genes reportedly regulated by DnaA were significantly altered between the wild type and Δ*diaA* Δ*hda* strains. However, further analysis of the genes whose levels were significantly altered using the PheNetic tool (De Maeyer *et al.*, 2013) revealed that expression of the majority was controlled by a handful of transcriptional regulators. For example, 39 of the 69 genes (57%) whose expression level was altered at least 4-fold in the Δ*diaA* strain are regulated by RpoH, RpoE, RpoS, Lrp, ArcA or Crp (Fig. S4A), while 66 of the 105 (63%) altered genes in the Δ*diaA* Δ*hda* strain are regulated by RpoH, RpoE, RpoS, Lrp, ArcA, Fis, NanR or PaaX (Fig. S4B). Although many of the observed changes were attributable to Δ*diaA*, we were struck by the fact that several RpoH-regulated genes were up regulated specifically in the Δ*diaA* Δ*hda* strain (Fig. 4A). This, taken together with the fact that the Δ*hda* strain was cold sensitive for growth, prompted us to ask whether induction of the heat shock response contributed to growth of the Δ*hda* strain. In addition to elevated temperature, a variety of external agents including ethanol induce the heat shock response by increasing the level of misfolded proteins (Bukau, 1993). Based on results of our quantitative transduction assay, addition of 4% ethanol to the growth medium efficiently suppressed Δ*hda* cold sensitivity (Fig. 4B). Similar results were observed using a quantitative spot assay (Fig. 4C). Ethanol also reduced the *oriC/terC* ratio of the Δ*hda* strain to near wild type levels (Fig. 5A). The reduced *oriC/terC* ratio was the result of less frequent initiation events, as measured by replication run-out using flow cytometry (Fig. 5, compare panels B and C). Although we cannot exclude the possibility that ethanol might denature one or more initiation factors, these results nevertheless suggest that induction of the heat shock response improves growth of strains lacking Δ*hda* function.

***diaA*, *yihG* and *polA* moderate *nrdAB* transcription to influence dNTP levels**

Since DnaA-ATP contributes to the regulation of *nrdAB* transcription (Augustin *et al.*, 1994, Jacobson & Fuchs, 1998, Gon *et al.*, 2006, Olliver *et al.*, 2010), we compared the RNA-seq expression levels of the various *nrd* genes between the wild type, Δ*diaA* and Δ*diaA* Δ*hda* strains. Although not significant, RNA-seq indicated that levels of *nrdAB* and *nrdDG* (class III RNR) were increased in the Δ*diaA* strain compared to the wild type RNA-seq control, while *nrdHIEF* (class IB RNR) were reduced (Fig. 6A). The opposite trend was observed in the Δ*diaA* Δ*hda* strain: *nrdAB* levels were reduced, while *nrdHIEF* levels were increased, as if to compensate for the reduction in *nrdAB*. In both cases, levels of the *nrdR* RNR transcriptional repressor were largely unaffected. In light of these findings, we used qPCR to measure *nrdA* and *nrdB* levels in these same strains, as well as the unsuppressed Δ*hda* strain (JCB100u1). Transcript levels of *nrdA*, and to a slightly lesser extent *nrdB*, were increased in the Δ*diaA* strain compared to the wild type control (Fig. 6B & C). In contrast, levels of both *nrdA* and *nrdB* were significantly reduced in the Δ*diaA* Δ*hda* as well as the unsuppressed Δ*hda* strain. Thus, the slight increase in *nrdA* and *nrdB* transcription observed in the Δ*diaA* strain was completely dependent on *hda* function (Fig. 6A–C). Taken together, these findings support the proposed role for Hda in regulating *nrdAB* transcription through RIDA (Olliver *et al.*, 2010, Gon *et al.*, 2006, Augustin *et al.*, 1994, Jacobson & Fuchs, 1998), and suggest a novel role for DiaA in regulating *nrdAB* expression (see Discussion).

Since *nrdAB* levels were modestly increased in the Δ*diaA* strain, we next asked whether suppression by multi-copy *yihG'-polA* also involved *nrdAB*. Compared to the wild type control, *nrdA* and *nrdB* transcript levels were elevated ~2-fold in the pRM100-bearing strain (Fig. 7A & B). As with Δ*diaA*, this increase was dependent on *hda* function, although the Δ*hda* pRM100 strain nevertheless expressed *nrdAB* at levels higher than the Δ*hda* strain (Fig. 7A & B). Consistent with their respective *nrdAB* transcript levels, Western blot analysis confirmed that NrdB protein levels were reduced in the two unsuppressed Δ*hda* strains, and increased in the Δ*diaA* and pRM100 strains (Fig. S5).

As an independent measure of NrdAB levels we used the tyrosyl radical scavenger hydroxyurea (HU), which specifically inhibits NrdB function (Fuchs & Karlstrom, 1973, Kren & Fuchs, 1987). HU sensitivity was measured by spotting serial dilutions of liquid cultures onto agar plates containing the indicated concentration of HU followed by overnight incubation at 37°C. Compared to the wild type control, the unsuppressed Δ*hda* strain was hypersensitive to HU (Fig. 6D), consistent with its relative NrdB level (Figs. 6C & S5). Since HU sensitivity was also described for the Δ*seqA* strain, due to its inability to support the elevated number of replication forks resulting form hyper-initiation (Sutera & Lovett, 2006), we compared HU sensitivity of isogenic Δ*hda* and Δ*seqA* strains. Since both Δ*hda* and Δ*seqA* strains hyper-initiate, but the Δ*hda* strain additionally expresses significantly reduced levels of *nrdAB*, we hypothesized that the Δ*hda* strain would be more sensitive to HU compared to Δ*seqA*. As summarized in Fig. S6, HU sensitivity of the Δ*hda* strain was more pronounced than that of the Δ*seqA* strain, arguing that this phenotype could be used as a proxy for NrdB activity. In contrast to the Δ*hda* strain, the Δ*diaA* strain was HU resistant compared to the wild type control (Fig. 6D), consistent with its modestly elevated levels of *nrdAB* expression. The increased HU resistance of the Δ*diaA* strain was dependent on *hda* function, as it was not observed with the Δ*diaA* Δ*hda* strain, which instead resembled the unsuppressed Δ*hda* strain (Fig. 6D). Overexpression of either *yihG* or *polA* alone was sufficient to confer HU resistance (Fig. 7C). Taken together, these results support the conclusion that *nrdAB* levels or NrdAB activity is increased in the strains bearing Δ*diaA* or pRM100.

Results discussed above demonstrate that loss of *diaA* function or overexpression of *nrdAB* or *yihG*'*-polA* serves to increase *nrdAB* transcript levels, suggesting these strains contain increased levels of DNA precursors. To confirm this, we directly measured relative levels of the individual dNTPs in the suppressed strains to determine whether suppression of Δ*hda* correlated with an increase in the levels of one or more of the 4 dNTPs. Loss of *hda* function resulted in reduced levels of all 4 dNTP, particularly dGTP and dATP (Fig. 8). Consistent with these findings, Fujimitsu *et al.* (Fujimitsu *et al.*, 2008) previously reported that dCTP levels were significantly reduced in the *hda-185* strain following a shift in growth from 42° to 25°C. In contrast to the Δ*hda* strain, loss of *diaA* function conferred a modest increase in both dGTP and dATP compared to wild type, while pRM100 conferred a significant increase in dATP. Importantly, dGTP and dATP levels in the Δ*diaA* Δ*hda* double mutant were similar to those observed for the wild type control, while dCTP and, to a lesser extent dTTP levels remained low. Although dGTP levels were still reduced in the Δ*hda* pRM100 strain, dATP levels were restored to wild type levels. These results, taken together with those discussed above, suggest that Δ*diaA* or overexpression of *yihG* or *polA* suppress Δ*hda* cold sensitivity by restoring the dNTP pool to near wild type levels. Elevated levels of YihG/Pol I increase dNTP levels by enhancing *nrdAB* transcription in the Δ*hda* strain, while Δ*diaA* acts via a different mechanism.

dNTP levels are affected by temperature and *hda* function

Results discussed above support the conclusion that suppression of Δ*hda* cold sensitivity by the different *sch* alleles involved their respective abilities to restore cellular dNTPs to near wild type levels. However, the relationship between these *sch* alleles and the heat shock response, which also suppressed Δ*hda* cold sensitivity (Fig. 6), was unclear. We hypothesized that NrdAB activity may be attenuated at lower growth temperatures. As a test of this hypothesis, we compared respective levels of HU sensitivity of isogenic wild type, Δ*diaA*, Δ*diaA* Δ*hda* and unsuppressed Δ*hda* strains at 30° and 37°C. Consistent with our hypothesis, the wild type strain was significantly more sensitive to HU when grown at 30°C compared to 37°C (Fig. 6D & E, compare 5 mM HU panels). Likewise, a comparable enhancement in the levels of HU sensitivity at 30° compared to 37°C was observed for the other strains. Based on results of qPCR (Fig. 9D), *nrdAB* transcript levels were comparable for the wild type strain grown at 30° or 37°C. As a control to confirm that HU sensitivity was directly proportional to NrdB levels, we measured HU sensitivity of wild type and Δ*hda* strains overexpressing NrdAB by virtue of plasmid pTKM226. As expected, overexpression of NrdAB at 37°C provided strong resistance to HU for both the wild type and Δ*hda* strains (Fig. 9A). However, at 30°C, overexpression of NrdAB provided only modest protection to the Δ*hda* strain (Fig. 9B). Enhanced HU sensitivity of the Δ*hda* strain bearing pTKM226 at 30°C was not the result of a failure to overexpress NrdAB, since both NrdB protein and *nrdA* transcript levels were comparable to those of the wild type control strain grown at 37°C (Fig. 9C & D). Taken together, these findings suggest that low temperature attenuates the activity of NrdAB.

We next measured dNTP levels in strains grown at 30° or 37°C to see if they differed as suggested by their respective levels of HU sensitivity. We first examined the wild type strain bearing the pBR322 control plasmid. With the exception of dATP, which was slightly elevated at 30° compared to 37°C, levels of the other dNTPs were similar regardless of whether the strain was grown at 30° or 37°C (Fig. 10). Nevertheless, it is possible that dNTP levels differ at 30° compared to 37°C following HU treatment, possibly explaining the enhance HU sensitivity observed for the wild type strain at 30° compared to 37°C (Fig. 6D & E). We next measured dNTP levels in the wild type and Δ*hda* strains bearing the *nrdAB*-expressing plasmid pTKM226. With the exception of dGTP, which was unchanged, levels of each of the other 3 dNTPs were increased in the wild type strain overexpressing *nrdAB* compared to the pBR322 control (Fig. 10). However, in contrast to the pBR322 control, relative dNTP levels in the NrdAB overexpressing strain differed as a function of the growth temperature: dCTP and dTTP levels were reduced at 30° compared to 37°C, while dATP was slightly elevated at 30° compared to 37°C. A very different profile was observed for the Δ*hda* strain overexpressing NrdAB: whereas dCTP and dATP levels were unaffected by growth temperature, dGTP was elevated at 30°C, while dTTP was elevated at 37°C (Fig. 10). In addition, dCTP levels were elevated more than 2-fold in the Δ*hda* strain grown at 30°C compared to the wild type control, while levels of each of the other 3 dNTPs were reduced. Although results discussed above support the conclusion that growth temperature influences dNTP levels they failed to demonstrate a reduction in the dNTP pool at 30° compared to 37°C in MG1655 expressing physiological levels of NrdAB. However, loss of *hda* function resulted in significant differences in the dNTP levels for the strain overexpressing NrdAB, suggesting a role for Hda in attenuating NrdAB activity.

Expression of the Fur and OxyR regulons is altered in the absence of *hda* function

In addition to inactivating NrdB, exposure of *E. coli* to HU stimulates iron uptake, leading to the production of hydroxyl radicals that contribute to cell death (Davies *et al.*, 2009). Since HU and Δ*hda* have in common the ability to reduce the level of active NrdAB within the cell, we asked whether iron regulation was affected in the Δ*hda* strain. The Fur protein regulates *E. coli* iron levels (Hantke, 1981). Under iron-replete conditions, Fur represses several genes involved in iron import, while under iron-deplete conditions the Fur regulon is derepressed, accelerating iron import. Based on our RNA-seq data, expression levels of Fur regulated genes were decreased in the Δ*diaA* strain compared to the wild type control (Fig. 11A). In contrast, levels of these same genes were increased in the Δ*diaA* Δ*hda* strain. We therefore used qPCR to measure levels of the Fur-regulated *fepD* transcript in both these and the unsuppressed Δ*hda* strain (JCB100u1). As summarized in Fig. 11B, levels were modestly increased in the Δ*diaA* Δ*hda* strain compared to the wild type control, but were ~5-fold elevated in the unsuppressed Δ*hda* strain, indicating the Fur regulon was derepressed in the absence of *hda* function.

Derepression of the Fur regulon leads to increased iron transport, which could help promote production of hydroxyl radicals via Fenton chemistry, contributing to the generation of oxidized DNA precursors, particularly 8-oxo-dG, which contributes to the 37°C Δ*hda* growth defect (Charbon *et al.*, 2014). In light of these findings, we hypothesized that excess iron may contribute to Δ*hda* cold sensitivity. Iron chelators act to reduce cellular iron levels, effectively protecting cells against formation of hydroxyl radicals. We therefore asked if the addition of iron chelators to the growth media suppressed Δ*hda* cold sensitivity. Based on results of plating assays, both dipyridyl and EDDHA suppressed Δ*hda* cold sensitivity (Fig. 11C). Likewise, addition of dipyridyl to the medium suppressed Δ*hda* cold sensitivity as measured by our quantitative transduction assay (Fig. 11D). Based on results of flow cytometry and qPCR, dipyridyl suppressed Δ*hda* by reducing the number of initiation events (Fig. 5, compare panels B & D), such that the *oriC/terC* ratio was near wild type levels (Fig. 5A).

To determine whether the response to oxidative stress was altered in the Δ*hda* strain, we compared expression levels of genes regulated by the oxidative stress response regulator OxyR (Christman *et al.*, 1985). Based on RNA-seq, several OxyR-regulated genes were modestly repressed in the Δ*diaA* Δ*hda* strain compared to the wild type and Δ*diaA* controls (Fig. 12A). To confirm this result, we used qPCR to measure levels of *katG*, which encodes the OxyR-regulated catalase, KatG (Morgan *et al.*, 1986). While *katG* levels were largely unchanged in the Δ*diaA* and Δ*diaA* Δ*hda* strains compared to the wild type control, they were ~4-fold reduced in the unsuppressed Δ*hda* strain (Fig. 12B). We next asked whether addition to the growth media of the hydroxyl radical scavenger thiourea suppressed Δ*hda* cold sensitivity. Addition of thiourea sensitized the Δ*diaA* and unsuppressed Δ*hda* strains at 37°C (Fig. 12C), yet significantly improved growth of the unsuppressed Δ*hda* strain at 30°C (Fig. 12D). While we do not understand the thiourea sensitivity at 37°C, these results support the view that increased levels of hydroxyl radicals contribute to *Δhda* cold sensitivity. Addition of DTT or cysteine to the growth media similarly suppressed Δ*hda* cold sensitivity, without affecting growth at 37°C, while addition of cystine did not (Fig. S7). These results demonstrate that suppression of Δ*hda* cold sensitivity relied on the redox activity of cysteine. Findings discussed above are consistent with published results indicating the 37°C growth defect of the Δ*hda* strain was suppressed by addition of reduced glutathione (GSH) to the growth media (Charbon *et al.*, 2014).

mutM **and** ***rnhB*** **function contribute to Δ*hda* cold sensitivity**

Poor growth of Δ*hda* strains at 37°C is due in part to dsDNA breaks caused by convergence of replication forks with ssDNA breaks resulting from MutM-catalyzed excision of 8-oxo-dG from nascent DNA (Charbon *et al.*, 2014). We used our quantitative transduction assay to determine whether the Δ*mutM* allele suppressed Δ*hda* cold sensitivity. As summarized in Fig. 2A, Δ*mutM* suppressed Δ*hda* cold sensitivity. Ribonucleotides are the most common lesion in DNA (Williams & Kunkel, 2014). Although DNA polymerases discriminate against ribonucleotides, rNTPs are present at ~100-fold higher levels than dNTPs (Williams & Kunkel, 2014). Since dNTP levels are significantly reduced in the *hda* strain, we hypothesized that excision from nascent DNA of inappropriately incorporated ribonucleotides might also contribute to dsDNA breaks that impair its growth. We further hypothesized that since the Δ*hda* strain contained significantly reduced levels of dNTPs, it may be more prone to incorporating rNTPs into nascent DNA, repair of which might contribute to the residual dsDNA breaks observed by Charbon and colleagues in the Δ*mutM* Δ*hda* strain (Charbon *et al.*, 2014). Using our quantitative transduction assay, we asked whether Δ*rnhA* (RNase HI) or Δ*rnhB* (RNase HII) suppressed Δ*hda* cold sensitivity. As summarized in Fig. 2A, Δ*rnhB*, but not Δ*rnhA*, partially suppressed Δ*hda* cold sensitivity, presumably by impeding ribonucleotide excision repair. Although not statistically significant, these results provide further support for the model that ssDNA nicks generated by global DNA repair functions contribute to lethal DNA damage that collectively impairs growth of the Δ*hda* strain. Finally, based on RNA-seq, the Δ*diaA* Δ*hda* strain displayed a low level of chronic SOS induction (Fig. S8), except for *recN* that was significantly induced compared to the wild type control (Table S1), consistent with increased numbers of dsDNA breaks in strains lacking *hda* function.

DISCUSSION

The growth defect of the Δ*hda* strain is due primarily to low levels of intracellular DNA precursors

The goal of the work discussed in this report was to gain insight into the biological role(s) of Hda, specifically, why loss of *hda* function but not Δ*seqA* or Δ*datA* conferred a severe growth defect at 30°C. To this end, we used a genetic assay to select for suppressors of Δ*hda* cold sensitivity. Our genetic characterization of these suppressors supports the conclusion that insufficient levels of intracellular DNA precursors serves as a primary basis for Δ*hda* cold sensitivity. Consistent with this conclusion, the Beckwith lab described a role for Hda in coordinating derepression of *nrdAB* transcription with initiation of DNA replication (Gon *et al*., 2006, Augustin *et al*., 1994, Jacobson & Fuchs, 1998, Olliver *et al*., 2010). Furthermore, both the Beckwith and Katayama labs demonstrated that elevated levels of NrdAB expressed from a plasmid improved growth of the Δ*hda* and *hda-185* strains at 37° and 25°C, respectively (Fujimitsu *et al*., 2008, Gon *et al*., 2006). Thus, *hda* is distinguished from *seqA* and *datA* in that it acts to regulate both the initiation of DNA replication and *nrdAB* transcript levels. Whereas Hda is estimated to catalyze ~80% of DnaA-ATP hydrolysis, *datA* is thought to be responsible for the remaining ~20% (Kasho & Katayama, 2013). Thus, *datA* may also play a role in regulating *nrdAB* by contributing to the management of cellular DnaA-ATP levels. DNA precursor levels are critically important for cellular viability: lack of thymine or guanine results in a phenomenon termed thymineless or guanineless death, respectively (Itsko & Schaaper, 2014, Barner & Cohen, 1954, Ahmad *et al*., 1998). One of the contributing factors to lethality during thymine starvation is induction of death-by-recombination pathway catalyzed by *recF*, *recQ* and *recJ* during which non-resolvable recombinational intermediates are accumulated in an attempt to repair progressively growing DNA damage (Nakayama *et al*., 1985, Nakayama, 2005, Fonville *et al*., 2010). We therefore used our quantitative transduction assay to determine whether the growth defect of the Δ*hda* strain required *recQ* function, consistent with it possibly resulting from a response to depletion of dGTP and/or dATP. As summarized in Fig. S9, the Δ*recQ* allele failed to improve growth of the Δ*hda* strain at 30°C, and instead significantly reduced its viability at 37°C. Thus, although the poor growth phenotype of the Δ*hda* strain appears to be the result of the significantly reduced dNTP pool, reduced viability does not appear to be solely attributable to a thymineless death-like death mechanism. Finally, It is not yet clear whether RIDA takes place at the replication fork or on β clamps that accumulate on lagging strand in the wake of replication. Since Hda must interact physically with the β clamp in order to catalyze RIDA, the rate of hydrolysis of DnaA-ATP to DnaA-ADP, and thus the rate at which *nrdAB* transcription becomes derepressed, may be coordinated with ongoing replication such that dNTP levels increase under conditions in which elongation of replication is slowed or impaired. In these cases, Hda may gain more frequent access to β clamps, particularly if Pol III function is impaired.

Roles for *diaA*, *yihG* and *polA* in regulating *nrdAB* transcription

Results discussed in this report reveal previously unrecognized roles for *diaA*, *yihG* and *polA* in regulating intracellular dNTP levels. The *diaA* gene was originally identified as a suppressor of the cold sensitive *dnaAcos* mutant strain (Ishida *et al*., 2004). Since DiaA forms a stable complex with DnaA and facilitates the ordered binding of DnaA-ATP at *oriC* to facilitate initiation of DNA replication, suppression of *dnaAcos* by Δ*diaA* was presumed to result from an initiation defect conferred by Δ*diaA*, although its potential to modulate the function of DnaA on DNA was suggested (Ishida *et al*., 2004, Keyamura *et al*., 2007, Keyamura *et al*., 2009, Fujimitsu *et al*., 2008). Our results demonstrate that DiaA plays a biologically important role in regulating *nrdAB* transcription. It is possible that DiaA facilitates loading of DnaA-ATP at the *nrdA* promoter, similar to its role at *oriC* during initiation (Keyamura *et al*., 2007), to repress *nrdAB* transcription. Alternatively, DiaA may regulate the ability of DnaA-ATP bound to one or more DnaA boxes upstream of *nrdA* to repress *nrdAB* transcription. The Δ*diaA* allele also restored near normal levels of dNTPs to the Δ*diaA* Δ*hda* strain (Fig. 8). The ability of the Δ*diaA* allele to restore dNTP levels is unrelated to its ability to modulate *nrdAB* transcription, since *nrdAB* levels were similar in the Δ*hda* and Δ*diaA* Δ*hda* strains (Fig. 6B & C). Thus, DiaA appears able to attenuate cellular dNTP levels via both *hda*-dependent and *hda*-independent mechanisms. Further work is required in order to define these mechanisms.

Overexpression of either *yihG* or *polA* suppressed Δ*hda* cold sensitivity. The ability of elevated levels of Pol I to suppress Δ*hda* was specific to this Pol, as it was not observed for overexpression of the other *E. coli* Pols (Fig. 2B). Like Δ*diaA*, overexpression of the first 196 codons of *yihG*, together with the complete *polA* gene (pRM100), increased *nrdAB* levels, and restored the intracellular dATP concentration to wild type levels in the absence of *hda* function (Fig. 8). Although YihG was originally reported to possess poly(A) polymerase activity (Cao *et al*., 1996), a subsequent study determined that it lacked this activity (Mohanty & Kushner, 1999). Based on its sequence, YihG belongs to the 1-acyl-sn-glycerol-3-phosphate acyltransferase family, suggesting it may play a role in lipid biosynthesis. Regeneration of DnaA-ADP to DnaA-ATP relies on either DnaA-reactivating sequences termed DARS1 and DARS2 (Fujimitsu *et al*., 2009) or association of DnaA with acidic phospholipids (Castuma *et al*., 1993, Garner & Crooke, 1996). Thus, multi-copy *yihG* might act to suppress Δ*hda* by affecting the lipid composition or the fluidity of the inner membrane, which, in turn, may influence the level of DnaA-ATP available for regulation of *nrdAB* by retarding the rate of ADP release from DnaA. In contrast, Pol I binds inverted repeats and may influence the expression level of *nrdAB* by binding to REP164 (Repetitive Extragenic Palindromic Sequence 164), which is located between *nrdA* and *nrdB* (Gilson *et al*., 1990). Alternatively, elevated levels of Pol I might promote more efficient repair of ssDNA breaks. This, in turn, would limit the frequency with which replication forks converge on ssDNA breaks to generate dsDNA breaks in the Δ*hda* strain (Charbon *et al*., 2014). However, the inability of elevated levels of Pol II, IV or V to suppress Δ*hda* cold sensitivity suggests that Pol I suppression involves a more sophisticated mechanism. Finally, it is possible that Pol I, whose transcription is activated by DnaA-ATP (Quinones *et al*., 1997), attenuates the ability of DnaA-ATP to repress *nrdAB*.

Increased levels of dNTPs may help the Δ*hda* strain to cope with DNA damage

RNR expression is DNA damage responsive in both prokaryotes and eukaryotes, suggesting an increased level of dNTPs are important for efficient repair of damaged DNA (Elledge & Davis, 1990, Monje-Casas *et al*., 2001). Transformation of the Δ*hda* strain with pRM100 significantly increased dATP levels without significantly changing levels of dGTP (Fig. 8). This finding suggests that limiting levels of dATP impair growth of the Δ*hda* strain. Alternatively, oxidized adenine may contribute to dsDNA breaks in the Δ*hda* strain via MUG-mediated cleavage of 8-oxo-dAMP:dTMP base pairs (Talhaoui *et al*., 2013). On the other hand, the higher levels of dATP conferred by pRM100 may be protective of dG oxidation, effectively reducing the level of 8-oxo-dG to improve growth of the Δ*hda* strain. Further work is required to test these hypotheses. Finally, it is particularly intriguing that Pol I, a repair DNA polymerase, plays a role in attenuating *nrdAB* expression to modulate dNTP levels, particularly in light of the finding that elevated levels of dNTPs contribute to the ability of *E. coli* to tolerate DNA damage.

Elevated temperature suppresses the Δ*hda* growth defect

The Δ*hda* strain grows considerably better at 42°C than it does at 30°C (Baxter & Sutton, 2012). Likewise, sensitivity of *E. coli* to HU is more pronounced at 30° compared to 37°C, particularly for the Δ*hda* strain (Figs. 6 & 9). Taken together, these finding suggest that NrdAB activity is temperature dependent. Although we did not observe a remarkable difference in the levels of the individual dNTPs for the wild type strain grown at 30° compared to 37°C, we did observe significant differences in dNTP levels for strains overexpressing NrdAB. Specifically, levels of dCTP and dTTP were significantly lower at 30° compared to 37°C in the wild type strain overexpressing NrdAB, while dATP levels were slightly higher at 30° compared to 37°C (Fig. 10). In contrast, dGTP levels were higher at 30°C in the Δ*hda* strain overexpressing NrdAB, while dTTP levels were lower at 30° compared to 37°C. A very different result was observed for the Δ*hda* strain overexpressing NrdAB. When grown at 30°C, levels of dCTP were significantly higher compared to the wild type control, while levels of dGTP, dTTP and dATP were reduced compared to the wild type control. These findings demonstrate that growth temperature can affect dNTP levels in strains overexpressing NrdAB. Moreover, they suggest that NrdAB function is altered in the absence of *hda* function. Mutations affecting the tRNA thiolation pathway confer HU sensitivity (Nakayashiki *et al.*, 2013). Although NrdAB levels were reduced in these mutants, the intracellular redox was shifted toward the reduced state, suggesting NrdAB activity was enhanced due to more efficient reduction of the NrdB disulfide-bridge. Thus, it would be interesting to determine whether loss of *hda* function influences the intracellular redox state. Consistent with this possibility, we determined that addition of DTT or cysteine to the growth media suppressed Δ*hda* cold sensitivity. DTT and cysteine can functionally replace the loss of thioredoxins (Trx) and glutaredoxins (Grx) required for reduction of the disulfide-bridge in NrdA following each catalytic cycle (Ritz & Beckwith, 2001). Thus, the ability of DTT or cysteine to suppress Δ*hda* cold sensitivity may result from an improved efficiency of NrdA disulfide-bridge reduction, increasing the specific activity of NrdAB in the Δ*hda* strain, which could increase dNTP levels even if *nrdAB* transcription were repressed. Finally, we cannot rule out the possibility that cold sensitivity of the Δ*hda* strain is the result of reduced phospholipid fluidity at 30° compared to 37°C and 42°C. Interaction of DnaA-ADP with fluid phospholipid membranes promotes release of ADP, allowing DnaA to bind ATP (Castuma *et al.*, 1993). Thus, the steady-state level of DnaA-ATP may be reduced at 30° compared to 37°C due to less efficient regeneration of DnaA-ADP. In addition to inducing the heat shock response, ethanol exposure also results in a decreased in the lipid:protein ratio (Dombek & Ingram, 1984), leading to more ridged membrane structures. Thus, although our findings support the view that Δ*hda* cold sensitivity is the result of reduced RNR activity, it is possible that cold sensitivity is instead the result of reduced steady-state levels of DnaA-ATP.

The Δ*hda* strain has several phenotypes in common with those induced by exposure of *E. coli* to HU

Exposure of *E. coli* to HU results in increased iron uptake and activation of the protein misfolding response (Davies *et al.*, 2009). Together, these events lead to formation of lethal levels of hydroxide radicals, which act to kill the cells. Since HU specifically inactivates NrdB (Fuchs & Karlstrom, 1973, Kren & Fuchs, 1987), while the Δ*hda* strain contains significantly reduced levels of NrdAB (Fig. S5), it is not surprising that the Δ*hda* strain has several phenotypes in common with HU-treated bacteria, including increased iron import (Fig. 11) and an altered OxyR response (Fig. 12). Our finding that Δ*hda* cold sensitivity was suppressed by addition to the growth media of iron chelators suggests that elevated iron levels contribute to the formation of reactive oxygen species in the Δ*hda* strain. Likewise, addition of thiourea, DTT or cysteine to the growth media suppressed Δ*hda* cold sensitivity, providing further support for the model that growth of the Δ*hda* strain is impaired by reactive oxygen species (Charbon *et al.*, 2014). While the unsuppressed Δ*hda* strain grows poorly (Riber *et al.*, 2006), it is nevertheless viable at temperatures equal to or greater than 37°C (Baxter & Sutton, 2012). We suggest that the Δ*hda* strain exhibits less severe phenotypes than cells treated with HU because of differences in NrdAB activity. Whereas HU has the ability at sufficiently high levels to inactivate the bulk of the cellular NrdB, *nrdAB* levels are reduced only ~2-fold in the Δ*hda* strain. Although we have not directly measured the fraction of active NrdAB in the Δ*hda* strain, there are sufficient levels to support growth at temperatures equal to or greater than 37°C. Finally, despite the fact that we did not observe a noticeable reduction in growth rate, it is possible that the ability of dipyridyl or cysteine to suppress Δ*hda* cold sensitivity resulted from a reduced frequency of initiation caused by slowed growth due to inhibition of general metabolism (Der Vartanian, 1988, Kari *et al.*, 1971).

Hda as a possible therapeutic target

Although *hda* is not widely conserved throughout the bacterial kingdom, it is present in several important pathogens in addition to *E. coli*, including *P. aeruginosa* (Winsor *et al.*, 2016). Foti and colleagues demonstrated that cytotoxicity of beta-lactams, quinolones and aminoglycosides results in part from lethal dsDNA breaks caused by efforts to repair closely spaced 8-oxo-dG lesions. As noted above, growth of the Δ*hda* strain is severely impaired by 8-oxo-dG (Charbon *et al.*, 2014). Thus, inactivation of *hda* function may synergize with traditional antimicrobial therapies, leading to more effective killing of certain human pathogens. We previously described a possible role for Hda in regulating access of TLS Pols to the replication fork (Baxter & Sutton, 2012). Foti and colleagues determined that Pol III, Pol IV and Pol V each contributed to incorporation of 8-oxo-dG in cells treated with antibiotics (Foti *et al.*, 2012). Thus, inactivation of *hda* may have the added benefit of enhancing access to the replication fork of TLS Pols (Baxter & Sutton, 2012), which may lead to more robust levels of 8-oxo-dG incorporation promoting more efficient cell killing.

EXPERIMENTAL PROCEDURES

Bacteriological techniques

Our laboratory *E. coli* MG1655 stock originally obtained from the CGSC was used as the strain background throughout this study. Strains were routinely cultured in LB (10 g/l Difco tryptone, 5 g/l Difco yeast extract, 10 g/l NaCl), unless otherwise indicated. When appropriate, the following antibiotics were used at the indicated concentrations: ampicillin (Amp), 150 µg/ml; chloramphenicol (Cam), 20 µg/ml; kanamycin (kan), 40 µg/ml. Strains were made using generalized P1*vir* transduction as described (Sutton, 2004), and are described in Table S2. Transformation of *E. coli* was performed using $CaCl_2$ competent cells as described (Sutton, 2004).

Identification and nucleotide sequence of suppressors of Δ*hda* cold sensitivity

Construction of cold-resistant Δ*hda*::*cat* suppressors was performed similarly to that previously described [29]. Briefly, transduction of the Δ*hda*::*cat* allele into strain MG1655 was performed through P1*vir* grown on strain ALO1917. Stable transductants were selected and cured of phage at 42°C on selective LB media, and independent transductants were struck out at 37°C to select for spontaneous suppressors. Healthy-growing clones were subsequently struck at both 30°C and 37°C on selective LB media to screen for suppression of cold-sensitivity. Isolates identified to grow uniformly well at both temperatures were selected for this study. In order to identify the genetic changes resultant in each suppressor, 1 ml of overnight culture from each strain grown in LB medium at 37°C was used to extract genomic DNA using Sigma™ GenElute™ Bacterial Genomic DNA kit. Samples were sequenced using 100-cycle paired-end sequencing on the Illumina Sequencing platform.

Transduction and susceptibility experiments

Transductions of Δ*hda*::*cat* were performed using P1*vir* grown on strain ALO1917 carrying the Δ*hda*::*cat* and *hsm*-1 (deletion of 2 thymines upstream of *seqA*) alleles. The *hsm*-1 (*seqA*) allele acts to suppress the growth defect of the Δ*hda* strain, and is unlinked to *hda*, allowing us to construct unsuppressed Δ*hda* mutant strains at 37° and 42°C, or to test the ability of other mutations to suppress Δ*hda* cold sensitivity at 30°C (Charbon *et al.*, 2011). Transductions were performed at 37°C as described previously by incubating the phage with the recipient cells in the presence of 5 mM calcium chloride for 20 minutes (Baxter & Sutton, 2012). This reaction was then mixed with top agar containing 500 mM sodium citrate and overlaid onto LB plates containing Cam. Plates were incubated at 42°C for 36 hrs, and at 30°C for 48 hrs. Transductions into the wild type at 42°C was included as a control for all experiments and the relative transduction efficiencies were calculated by normalizing to this condition. For susceptibility measurements, saturated cultures were serially diluted 10-fold and aliquots of these dilutions were spotted onto plates with or without the indicated chemical (see Figure legends). All chemical stocks were prepared fresh. Plates were photographed following incubation for 16 hrs at the indicated temperatures.

Quantitative PCR (qPCR) methods

For measuring *oriC* and *terC* copy numbers, cultures were grown at 37°C in LB medium to an OD_{600nm} of 0.5–0.6 unless noted otherwise. One-ml of this culture was spun down and genomic DNA was extracted from cell pellets using the Sigma™ GenElute™ Bacterial Genomic DNA kit as per the manufacturer's recommendation. Genomic DNA was used as template to perform qPCR using the primers (Table S2) that amplify 150 bp fragments near the origin (*mnmG*) or terminus (*dcp*), respectively, using Bio-Rad SsoAdvanced™ Universal SYBR® Green Supermix in Bio-Rad CFX96 Touch PCR equipment with manual Cq threshold of 60.

To measure mRNA levels, cells were grown as described above at the required temperature. Cells from 1 ml of exponential phase culture were pelleted and total RNA was extracted using phenol-chloroform followed by ethanol precipitation. Twelve-μg of RNA was treated with DNase I and re-extracted using the Qiagen RNeasy mini kit as per manufacturer's recommendations. One hundred-ng of DNase I treated RNA was used to generate cDNA using Bio-Rad iScript cDNA synthesis kit as per the manufacturer's recommendations. The resulting cDNA was used for qPCR with primers that produce ~100 bp fragments specific to the gene under study.

Flow cytometry

Genome content was measured using flow cytometry as described previously with some modifications (Baxter & Sutton, 2012). Results shown are representative of at least 2 independent experiments. Briefly, the cells were grown at 37°C in LB medium to OD_{600nm} 0.1–0.2, at which point rifampicin and cephalexin were added to 500 μg/ml and 25 μg/ml, respectively. Cultures were incubated at 37°C with aeration for 4 hrs. One-ml of each culture was then mixed with 9 ml of 70% ethanol prior to being fixed at 4°C for 48 hrs. Fixed cells were pelleted and resuspended in 100 μl of 50 mM Sodium Citrate, pH 7.0. RNA was removed by the addition of 0.25 mg/ml RNase A followed by incubation at 50°C for 1 hr. Cells were again pelleted and resuspended in 100 μl of 10 μM SYTOX® Green Nucleic Acid stain (Life Technologies) followed by incubation at room temperature for 2 hrs in the dark. The cells were then diluted 10-fold with 50 mM Sodium Citrate, pH 7.0, and analyzed using BD FACS Canto instrument and FlowJo® 10.2 Software.

Western blot analysis of NrdB protein levels

Overnight cultures of the indicated strains were sub-cultured 1:100 in LB to mid-exponential phase (OD_{600} ~0.5). Cell from 2 ml of culture were collected by centrifugation and the cell pellet was resuspended in 40 μl B-PER protein extraction reagent (Pierce). Eighty-μl of SDS loading dye (63mM Tris (pH 6.8), 10% glycerol, 2% SDS, 0.005% bromophenol blue, 10% 2-mercaptoethanol) was then added and the mixture was heated at 95°C for 10 min. Ten-μl of this sample was loaded into the wells of 12% SDS-PAGE gel. Proteins were resolved then transferred to polyvinylidene difluoride (PVDF) membrane using a Trans Blot Turbo semi-dry transfer apparatus (Bio-Rad). Membranes were treated with primary antibody (1:5,000 of rabbit anti-NrdB polyclonal) overnight at 4°C. After washing, the membrane was probed with secondary antibody (1:50,000 of goat anti-rabbit form Bio-Rad) for 1 hr, washed, treated with 2 ml of the West Dura substrate mixture (Thermo Scientific) for 2 min and visualized with a ChemiDoc imager (Bio-Rad).

Whole transcriptome analysis

The RNA required for whole transcriptome analysis was prepared as described above for quantitative PCR using phenol-chloroform from exponential phase cultures grown at 37°C and is then depleted of the ribosomal RNA (rRNA) using the Bacterial Ribo-Zero rRNA Removal Kit (Illumina) as per manufacturer's recommendations. Quality control for the extracted RNA was performed using a Bioanalyzer. Purified mRNA was used to perform RNA-seq as Rapid 100 cycle single read sequencing using the Illumina Next Generation Sequencer. Generation of FPKMs was performed using Cufflinks 2.1.1. The log_2-fold changes in FPKMs compared to wild types are then clustered using the Cluster 3.0 program with uncentered correlation similarity metric using average linkage clustering method. Images of the clusters were generated using the Java Tree view software package.

Nucleotide Extraction and HPLC analysis

Levels of the individual dNTPs were quantified essentially as described previously (Ahluwalia *et al.*, 2012). Briefly, cells from culture aliquots (120 ml) were harvested at OD_{630nm} = 0.5–0.6 by filtering through a 90-mm diameter polycarbonate membrane filter (0.4 µm pore size; Millipore). The filter was transferred to a Petri dish lid containing 10 ml of 60% aqueous methanol at -20°C. After overnight incubation at −20°C, the liquid and filter were removed to a 50 ml conical Falcon tube, vortexed, and centrifuged. After removal of the filter, the tube was placed in boiling water for 5 min, centrifuged for 15 min at 17,000 × g, and the supernatant lyophilized. After lyophilization the residue was dissolved in 750 µl sterile water and extracted with 500 µl of chloroform. The upper (water) phase was lyophilized again and the residue was dissolved in 90 µl sterile water. HPLC analysis of the extracted dNTPs was performed by reversed-phase chromatography on an Agilent 1100 high-pressure liquid chromatography instrument with UV detection at 254 nm. Nucleotides were separated on a Zorbax Eclipse XDBC18 3.5 µM (150 by 4.6 mm) column equipped with a Zorbax Eclipse XDBC18 guard column. At a flow rate of 0.8 ml/min, a linear gradient of 70:30 Buffer A to Buffer B was run to 40:60 over 30 min. The gradient was then changed over 60 min from 40:60:0 to 0:87.5:12.5 for Buffer A:Buffer B:Buffer C. To wash the column between samples the gradient was first changed from 0:87.5:12.5 to 0:70:30 over 10 minutes with a final stepwise change to 70:30:0 for an additional 20 min. Buffer A consisted of 5 mM tetrabutyl ammonium phosphate (PicA Reagent; Waters), 10 mM KH_2PO_4, and 0.25% methanol adjusted to pH 6.9. Buffer B consisted of 5 mM tetrabutyl ammonium phosphate, 50 mM KH_2PO_4, and 30% methanol (pH 7.0). Buffer C was acetonitrile. Peaks for individual dNTPs were identified based on retention times of dNTP standards and were further confirmed by the recorded UV spectra for each peak. dNTP standards were obtained from Sigma.

Supplementary Material

Refer to Web version on PubMed Central for supplementary material.

Acknowledgments

We thank Anders Løbner-Olesen (Roskilde University) and Martin Marinus (University of Massachusetts Medical School) for *E. coli* strain ALO1917, Tsutomu Katayama (Kyushu University) for plasmids pRM100, pTKM221 and pTKM226, JoAnne Stubbe (Massachusetts Institute of Technology) for the anti-NrdB polyclonal antibody, Steven Gill (University at Rochester) and the University at Buffalo Genomics Facility for help with RNA-seq experiments, Michael Nanfara for cloning plasmid pMN122 and transduction experiments summarized in Fig. 2B, Michelle Scotland for help with spotting experiments summarized in Fig. 7C, and the members of our labs for helpful discussions. This work was supported by Public Health Service Award R01 GM066094 from the NIGMS/National Institutes of Health (MDS) and the Intramural Research Program of the National Institutes of Health NIEHS project number Z01 ES065086 (RMS).

References

Ahluwalia D, Bienstock RJ, Schaaper RM. Novel mutator mutants of *E. coli nrdAB* ribonucleotide reductase: insight into allosteric regulation and control of mutation rates. DNA repair. 2012; 11:480–487. [PubMed: 22417940]

Ahmad SI, Kirk SH, Eisenstark A. Thymine metabolism and thymineless death in prokaryotes and eukaryotes. Annual review of microbiology. 1998; 52:591–625.

Augustin LB, Jacobson BA, Fuchs JA. *Escherichia coli* Fis and DnaA proteins bind specifically to the *nrd* promoter region and affect expression of an nrd-lac fusion. Journal of bacteriology. 1994; 176:378–387. [PubMed: 8288532]

Barner HD, Cohen SS. The induction of thymine synthesis by T2 infection of a thymine requiring mutant of *Escherichia coli*. Journal of bacteriology. 1954; 68:80–88. [PubMed: 13183905]

Baxter JC, Sutton MD. Evidence for roles of the *Escherichia coli* Hda protein beyond regulatory inactivation of DnaA. Molecular microbiology. 2012; 85:648–668. [PubMed: 22716942]

Braun RE, O'Day K, Wright A. Autoregulation of the DNA replication gene dnaA in E. coli K-12. Cell. 1985; 40:159–169. [PubMed: 2981626]

Bukau B. Regulation of the *Escherichia coli* heat-shock response. Molecular microbiology. 1993; 9:671–680. [PubMed: 7901731]

Cao GJ, Pogliano J, Sarkar N. Identification of the coding region for a second poly(A) polymerase in *Escherichia coli*. Proceedings of the National Academy of Sciences of the United States of America. 1996; 93:11580–11585. [PubMed: 8876178]

Carr KM, Kaguni JM. Stoichiometry of DnaA and DnaB protein in initiation at the *Escherichia coli* chromosomal origin. The Journal of biological chemistry. 2001; 276:44919–44925. [PubMed: 11551962]

Castuma CE, Crooke E, Kornberg A. Fluid membranes with acidic domains activate DnaA, the initiator protein of replication in *Escherichia coli*. The Journal of biological chemistry. 1993; 268:24665–24668. [PubMed: 8227025]

Charbon G, Bjorn L, Mendoza-Chamizo B, Frimodt-Moller J, Lobner-Olesen A. Oxidative DNA damage is instrumental in hyperreplication stress-induced inviability of *Escherichia coli*. Nucleic acids research. 2014; 42:13228–13241. [PubMed: 25389264]

Charbon G, Riber L, Cohen M, Skovgaard O, Fujimitsu K, Katayama T, Lobner-Olesen A. Suppressors of DnaA(ATP) imposed overinitiation in *Escherichia coli*. Molecular microbiology. 2011; 79:914–928. [PubMed: 21299647]

Chodavarapu S, Kaguni JM. Replication Initiation in Bacteria. The Enzymes. 2016; 39:1–30. [PubMed: 27241926]

Christman MF, Morgan RW, Jacobson FS, Ames BN. Positive control of a regulon for defenses against oxidative stress and some heat-shock proteins in *Salmonella typhimurium*. Cell. 1985; 41:753–762. [PubMed: 2988786]

Collier J, Shapiro L. Feedback control of DnaA-mediated replication initiation by replisome-associated HdaA protein in *Caulobacter*. Journal of bacteriology. 2009; 191:5706–5716. [PubMed: 19633089]

Crooke E, Thresher R, Hwang DS, Griffith J, Kornberg A. Replicatively active complexes of DnaA protein and the *Escherichia coli* chromosomal origin observed in the electron microscope. Journal of molecular biology. 1993; 233:16–24. [PubMed: 8377183]

Daley DO, Rapp M, Granseth E, Melen K, Drew D, von Heijne G. Global topology analysis of the *Escherichia coli* inner membrane proteome. Science. 2005; 308:1321–1323. [PubMed: 15919996]

Davies BW, Kohanski MA, Simmons LA, Winkler JA, Collins JJ, Walker GC. Hydroxyurea induces hydroxyl radical-mediated cell death in *Escherichia coli*. Molecular cell. 2009; 36:845–860. [PubMed: 20005847]

De Maeyer D, Renkens J, Cloots L, De Raedt L, Marchal K. PheNetic: network-based interpretation of unstructured gene lists in *E. coli*. Molecular bioSystems. 2013; 9:1594–1603. [PubMed: 23591551]

Der Vartanian M. Differences in excretion and efficiency of the aerobactin and enterochelin siderophores in a bovine pathogenic strain of *Escherichia coli*. Infection and immunity. 1988; 56:413–418. [PubMed: 2962945]

Dombek KM, Ingram LO. Effects of ethanol on the *Escherichia coli* plasma membrane. Journal of bacteriology. 1984; 157:233–239. [PubMed: 6360997]

Duderstadt KE, Chuang K, Berger JM. DNA stretching by bacterial initiators promotes replication origin opening. Nature. 2011; 478:209–213. [PubMed: 21964332]

Duderstadt KE, Mott ML, Crisona NJ, Chuang K, Yang H, Berger JM. Origin remodeling and opening in bacteria rely on distinct assembly states of the DnaA initiator. The Journal of biological chemistry. 2010; 285:28229–28239. [PubMed: 20595381]

Elledge SJ, Davis RW. Two genes differentially regulated in the cell cycle and by DNA-damaging agents encode alternative regulatory subunits of ribonucleotide reductase. Genes & development. 1990; 4:740–751. [PubMed: 2199320]

Feeney MA, Ke N, Beckwith J. Mutations at several loci cause increased expression of ribonucleotide reductase in *Escherichia coli*. Journal of bacteriology. 2012; 194:1515–1522. [PubMed: 22247510]

Fernandez-Fernandez C, Grosse K, Sourjik V, Collier J. The beta-sliding clamp directs the localization of HdaA to the replisome in *Caulobacter crescentus*. Microbiology. 2013; 159:2237–2248. [PubMed: 23974073]

Fonville NC, Bates D, Hastings PJ, Hanawalt PC, Rosenberg SM. Role of RecA and the SOS response in thymineless death in *Escherichia coli*. PLoS genetics. 2010; 6:e1000865. [PubMed: 20221259]

Foti JJ, Devadoss B, Winkler JA, Collins JJ, Walker GC. Oxidation of the guanine nucleotide pool underlies cell death by bactericidal antibiotics. Science. 2012; 336:315–319. [PubMed: 22517853]

Fuchs JA, Karlstrom HO. A mutant of *Escherichia coli* defective in ribonucleosidediphosphate reductase. 2. Characterization of the enzymatic defect. European journal of biochemistry/FEBS. 1973; 32:457–462.

Fujimitsu K, Senriuchi T, Katayama T. Specific genomic sequences of E. coli promote replicational initiation by directly reactivating ADP-DnaA. Genes & development. 2009; 23:1221–1233. [PubMed: 19401329]

Fujimitsu K, Su'etsugu M, Yamaguchi Y, Mazda K, Fu N, Kawakami H, Katayama T. Modes of overinitiation, *dnaA* gene expression, and inhibition of cell division in a novel cold-sensitive hda mutant of *Escherichia coli*. Journal of bacteriology. 2008; 190:5368–5381. [PubMed: 18502852]

Garner J, Crooke E. Membrane regulation of the chromosomal replication activity of *E. coli* DnaA requires a discrete site on the protein. The EMBO journal. 1996; 15:3477–3485. [PubMed: 8670850]

Gilson E, Perrin D, Hofnung M. DNA polymerase I and a protein complex bind specifically to *E. coli* palindromic unit highly repetitive DNA: implications for bacterial chromosome organization. Nucleic acids research. 1990; 18:3941–3952. [PubMed: 2197600]

Gon S, Camara JE, Klungsoyr HK, Crooke E, Skarstad K, Beckwith J. A novel regulatory mechanism couples deoxyribonucleotide synthesis and DNA replication in *Escherichia coli*. The EMBO journal. 2006; 25:1137–1147. [PubMed: 16482221]

Granseth E, Daley DO, Rapp M, Melen K, von Heijne G. Experimentally constrained topology models for 51,208 bacterial inner membrane proteins. Journal of molecular biology. 2005; 352:489–494. [PubMed: 16120447]

Hantke K. Regulation of ferric iron transport in *Escherichia coli* K12: isolation of a constitutive mutant. Molecular & general genetics: MGG. 1981; 182:288–292. [PubMed: 7026976]

Ishida T, Akimitsu N, Kashioka T, Hatano M, Kubota T, Ogata Y, Sekimizu K, Katayama T. DiaA, a novel DnaA-binding protein, ensures the timely initiation of *Escherichia coli* chromosome replication. The Journal of biological chemistry. 2004; 279:45546–45555. [PubMed: 15326179]

Itsko M, Schaaper RM. dGTP starvation in *Escherichia coli* provides new insights into the thymineless-death phenomenon. PLoS genetics. 2014; 10:e1004310. [PubMed: 24810600]

Jacobson BA, Fuchs JA. Multiple cis-acting sites positively regulate *Escherichia coli nrd* expression. Molecular microbiology. 1998; 28:1315–1322. [PubMed: 9680219]

Joyce CM, Kelley WS, Grindley ND. Nucleotide sequence of the *Escherichia coli polA* gene and primary structure of DNA polymerase I. The Journal of biological chemistry. 1982; 257:1958–1964. [PubMed: 6276402]

Kaguni JM. DnaA: controlling the initiation of bacterial DNA replication and more. Annual review of microbiology. 2006; 60:351–375.

Kari C, Nagy Z, Kovacs P, Hernadi F. Mechanism of the growth inhibitory effect of cysteine on *Escherichia coli*. Journal of general microbiology. 1971; 68:349–356. [PubMed: 4944587]

Kasho K, Katayama T. DnaA binding locus *datA* promotes DnaA-ATP hydrolysis to enable cell cycle-coordinated replication initiation. Proceedings of the National Academy of Sciences of the United States of America. 2013; 110:936–941. [PubMed: 23277577]

Katayama T, Kubota T, Kurokawa K, Crooke E, Sekimizu K. The initiator function of DnaA protein is negatively regulated by the sliding clamp of the *E. coli* chromosomal replicase. Cell. 1998; 94:61–71. [PubMed: 9674428]

Katayama T, Ozaki S, Keyamura K, Fujimitsu K. Regulation of the replication cycle: conserved and diverse regulatory systems for DnaA and *oriC*. Nature reviews Microbiology. 2010; 8:163–170. [PubMed: 20157337]

Kato J, Katayama T. Hda, a novel DnaA-related protein, regulates the replication cycle in *Escherichia coli*. The EMBO journal. 2001; 20:4253–4262. [PubMed: 11483528]

Kawakami H, Katayama T. DnaA, ORC, and Cdc6: similarity beyond the domains of life and diversity. Biochemistry and cell biology = Biochimie et biologie cellulaire. 2010; 88:49–62. [PubMed: 20130679]

Keyamura K, Abe Y, Higashi M, Ueda T, Katayama T. DiaA dynamics are coupled with changes in initial origin complexes leading to helicase loading. The Journal of biological chemistry. 2009; 284:25038–25050. [PubMed: 19632993]

Keyamura K, Fujikawa N, Ishida T, Ozaki S, Su’etsugu M, Fujimitsu K, Kagawa W, Yokoyama S, Kurumizaka H, Katayama T. The interaction of DiaA and DnaA regulates the replication cycle in *E. coli* by directly promoting ATP DnaA-specific initiation complexes. Genes & development. 2007; 21:2083–2099. [PubMed: 17699754]

Kitagawa R, Mitsuki H, Okazaki T, Ogawa T. A novel DnaA protein-binding site at 94.7 min on the *Escherichia coli* chromosome. Molecular microbiology. 1996; 19:1137–1147. [PubMed: 8830270]

Kren B, Fuchs JA. Characterization of the *ftsB* gene as an allele of the *nrdB* gene in *Escherichia coli*. Journal of bacteriology. 1987; 169:14–18. [PubMed: 3025167]

Kucherer C, Lother H, Kolling R, Schauzu MA, Messer W. Regulation of transcription of the chromosomal *dnaA* gene of *Escherichia coli*. Molecular & general genetics: MGG. 1986; 205:115–121. [PubMed: 3025553]

Leonard AC, Grimwade JE. Initiation of DNA Replication. EcoSal Plus. 2010; 4

Leonard AC, Grimwade JE. Regulation of DnaA assembly and activity: taking directions from the genome. Annual review of microbiology. 2011; 65:19–35.

Lu M, Campbell JL, Boye E, Kleckner N. SeqA: a negative modulator of replication initiation in *E. coli*. Cell. 1994; 77:413–426. [PubMed: 8011018]

Margulies C, Kaguni JM. Ordered and sequential binding of DnaA protein to *oriC*, the chromosomal origin of *Escherichia coli*. The Journal of biological chemistry. 1996; 271:17035–17040. [PubMed: 8663334]

Marszalek J, Kaguni JM. DnaA protein directs the binding of DnaB protein in initiation of DNA replication in *Escherichia coli*. The Journal of biological chemistry. 1994; 269:4883–4890. [PubMed: 8106460]

Messer W, Weigel C. DnaA initiator–also a transcription factor. Molecular microbiology. 1997; 24:1–6. [PubMed: 9140960]

Mohanty BK, Kushner SR. Residual polyadenylation in poly(A) polymerase I (*pcnB*) mutants of *Escherichia coli* does not result from the activity encoded by the *f310* gene. Molecular microbiology. 1999; 34:1109–1119. [PubMed: 10594834]

Monje-Casas F, Jurado J, Prieto-Alamo MJ, Holmgren A, Pueyo C. Expression analysis of the *nrdHIEF* operon from *Escherichia coli*. Conditions that trigger the transcript level in vivo. The Journal of biological chemistry. 2001; 276:18031–18037. [PubMed: 11278973]

Morgan RW, Christman MF, Jacobson FS, Storz G, Ames BN. Hydrogen peroxide-inducible proteins in *Salmonella typhimurium* overlap with heat shock and other stress proteins. Proceedings of the National Academy of Sciences of the United States of America. 1986; 83:8059–8063. [PubMed: 3534881]

Nakayama H. *Escherichia coli* RecQ helicase: a player in thymineless death. Mutation research. 2005; 577:228–236. [PubMed: 15922367]

Nakayama K, Irino N, Nakayama H. The *recQ* gene of *Escherichia coli* K12: molecular cloning and isolation of insertion mutants. Molecular & general genetics: MGG. 1985; 200:266–271. [PubMed: 2993821]

Nakayashiki T, Saito N, Takeuchi R, Kadokura H, Nakahigashi K, Wanner BL, Mori H. The tRNA thiolation pathway modulates the intracellular redox state in *Escherichia coli*. Journal of bacteriology. 2013; 195:2039–2049. [PubMed: 23457245]

Nievera C, Torgue JJ, Grimwade JE, Leonard AC. SeqA blocking of DnaA-*oriC* interactions ensures staged assembly of the *E. coli* pre-RC. Molecular cell. 2006; 24:581–592. [PubMed: 17114060]

Olliver A, Saggioro C, Herrick J, Sclavi B. DnaA-ATP acts as a molecular switch to control levels of ribonucleotide reductase expression in *Escherichia coli*. Molecular microbiology. 2010; 76:1555–1571. [PubMed: 20487274]

Ortenberg R, Gon S, Porat A, Beckwith J. Interactions of glutaredoxins, ribonucleotide reductase, and components of the DNA replication system of *Escherichia coli*. Proceedings of the National Academy of Sciences of the United States of America. 2004; 101:7439–7444. [PubMed: 15123823]

Quinones A, Wandt G, Kleinstauber S, Messer W. DnaA protein stimulates *polA* gene expression in *Escherichia coli*. Molecular microbiology. 1997; 23:1193–1202. [PubMed: 9106210]

Riber L, Olsson JA, Jensen RB, Skovgaard O, Dasgupta S, Marinus MG, Lobner-Olesen A. Hda-mediated inactivation of the DnaA protein and *dnaA* gene autoregulation act in concert to ensure homeostatic maintenance of the *Escherichia coli* chromosome. Genes & development. 2006; 20:2121–2134. [PubMed: 16882985]

Ritz D, Beckwith J. Roles of thiol-redox pathways in bacteria. Annual review of microbiology. 2001; 55:21–48.

Seitz H, Weigel C, Messer W. The interaction domains of the DnaA and DnaB replication proteins of *Escherichia coli*. Molecular microbiology. 2000; 37:1270–1279. [PubMed: 10972842]

Simmons LA, Breier AM, Cozzarelli NR, Kaguni JM. Hyperinitiation of DNA replication in *Escherichia coli* leads to replication fork collapse and inviability. Molecular microbiology. 2004; 51:349–358. [PubMed: 14756777]

Slater S, Wold S, Lu M, Boye E, Skarstad K, Kleckner N. E. coli SeqA protein binds *oriC* in two different methyl-modulated reactions appropriate to its roles in DNA replication initiation and origin sequestration. Cell. 1995; 82:927–936. [PubMed: 7553853]

Su'etsugu M, Shimuta TR, Ishida T, Kawakami H, Katayama T. Protein associations in DnaA-ATP hydrolysis mediated by the Hda-replicase clamp complex. The Journal of biological chemistry. 2005; 280:6528–6536. [PubMed: 15611053]

Su'etsugu M, Takata M, Kubota T, Matsuda Y, Katayama T. Molecular mechanism of DNA replication-coupled inactivation of the initiator protein in *Escherichia coli*: interaction of DnaA with the sliding clamp-loaded DNA and the sliding clamp-Hda complex. Genes to cells: devoted to molecular & cellular mechanisms. 2004; 9:509–522. [PubMed: 15189445]

Sutera VA Jr, Lovett ST. The role of replication initiation control in promoting survival of replication fork damage. Molecular microbiology. 2006; 60:229–239. [PubMed: 16556234]

Sutton MD. The *Escherichia coli dnaN159* mutant displays altered DNA polymerase usage and chronic SOS induction. Journal of bacteriology. 2004; 186:6738–6748. [PubMed: 15466025]

Sutton MD, Carr KM, Vicente M, Kaguni JM. *Escherichia coli* DnaA protein. The N-terminal domain and loading of DnaB helicase at the *E. coli* chromosomal origin. The Journal of biological chemistry. 1998; 273:34255–34262. [PubMed: 9852089]

Talhaoui I, Couve S, Ishchenko AA, Kunz C, Schar P, Saparbaev M. 7,8-Dihydro-8-oxoadenine, a highly mutagenic adduct, is repaired by *Escherichia coli* and human mismatch-specific uracil/thymine-DNA glycosylases. Nucleic acids research. 2013; 41:912–923. [PubMed: 23209024]

Urbonavicius J, Jager G, Bjork GR. Amino acid residues of the *Escherichia coli* tRNA(m5U54)methyltransferase (TrmA) critical for stability, covalent binding of tRNA and enzymatic activity. Nucleic acids research. 2007; 35:3297–3305. [PubMed: 17459887]

Wang QP, Kaguni JM. Transcriptional repression of the *dnaA* gene of *Escherichia coli* by dnaA protein. Molecular & general genetics: MGG. 1987; 209:518–525. [PubMed: 2828882]

Wang QP, Kaguni JM. dnaA protein regulates transcriptions of the *rpoH* gene of *Escherichia coli*. The Journal of biological chemistry. 1989; 264:7338–7344. [PubMed: 2540187]

Williams JS, Kunkel TA. Ribonucleotides in DNA: origins, repair and consequences. DNA repair. 2014; 19:27–37. [PubMed: 24794402]

Winsor GL, Griffiths EJ, Lo R, Dhillon BK, Shay JA, Brinkman FS. Enhanced annotations and features for comparing thousands of Pseudomonas genomes in the Pseudomonas genome database. Nucleic acids research. 2016; 44:D646–653. [PubMed: 26578582]

Wold S, Boye E, Slater S, Kleckner N, Skarstad K. Effects of purified SeqA protein on *oriC*-dependent DNA replication in vitro. The EMBO journal. 1998; 17:4158–4165. [PubMed: 9670030]

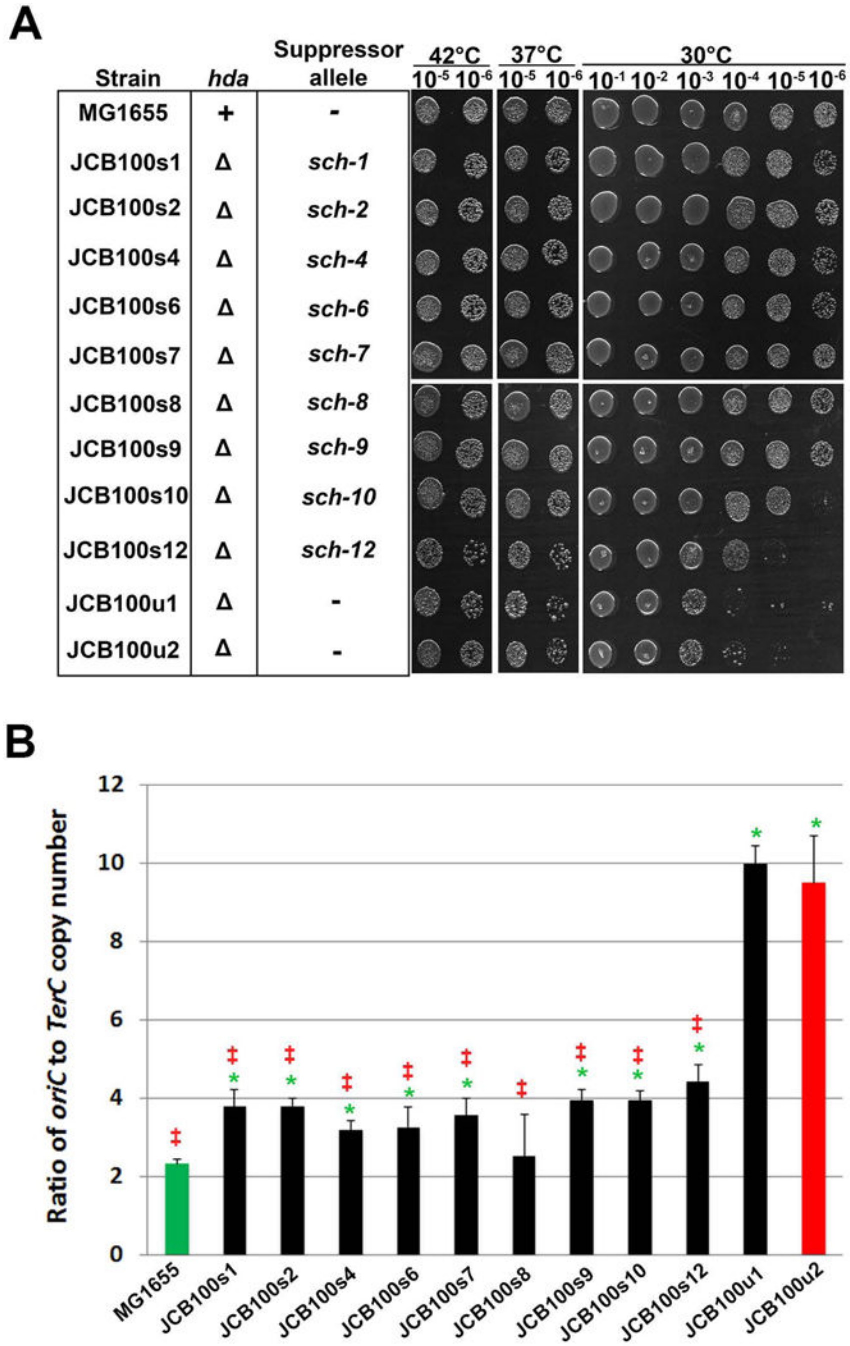

Figure 1. Phenotypes of suppressors (*sch* alleles) of cold sensitive Δ*hda*

(A) The ability of suppressed strains to grow at 30°, 37° and 42°C was measured using a quantitative spot assay, and **(B)** *oriC*/*terC* copy number ratios were measured using qPCR, as described in Experimental Procedures. The ability of the suppressed strains to grow at the indicated temperatures was measured 3 times, and representative results are shown. Values summarized in panel B represent the average of 3 determinations ± one standard deviation. Symbols are as follows: ‡, $p < 0.05$ relative to JCB100u2 (red); *, $p < 0.05$ relative to MG1655 (green).

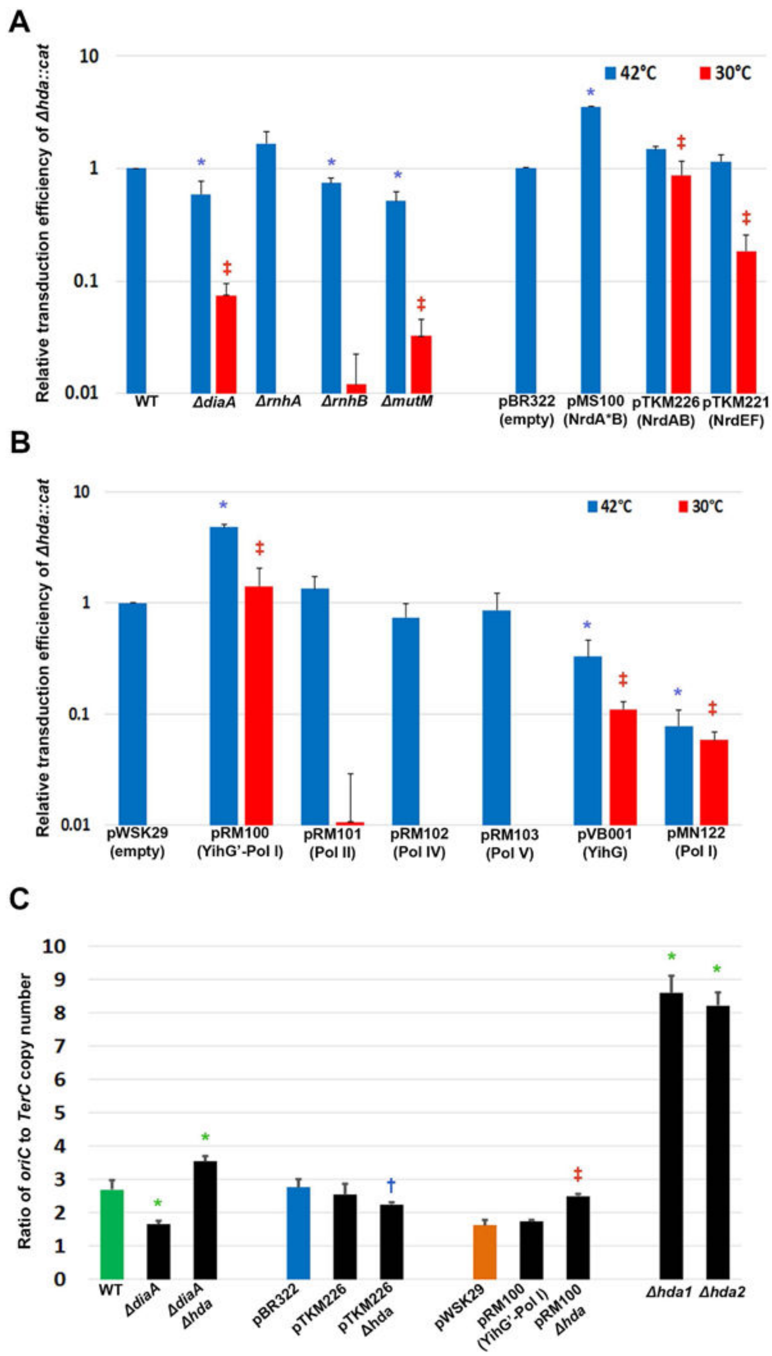

Figure 2. Respective abilities of the different *sch* alleles to suppress Δ*hda* cold sensitivity

(A & B) The respective ability of each indicated allele to suppress Δ*hda* cold sensitivity was measured using a quantitative Δ*hda*::*cat* P1*vir* transduction assay, and **(C)** *oriC*/*terC* copy number ratios were measured using qPCR, as described in Experimental Procedures. Transduction frequencies are normalized to the wild type (WT) control bearing the empty vector and grown at 42°C, which was set equal to 1.0. The actual range of transduction frequencies observed was 10^{-6}–10^{-8} CFU/PFU. Results in panels A-C represent the average of at least 3 determinations ± one standard deviation. Symbols are as follows: In panels A &

B; blue *, $p < 0.05$ relative to control at 42°C (control is WT for Δ*diaA*, Δ*rnhA*, Δ*rnhB* and Δ*mutM* or empty vector for the plasmid variants). Red ‡, $p < 0.05$ relative to controls at 30°C; in panel C; green *, $p < 0.05$ relative to WT. Blue †, $p < 0.05$ relative to pBR322; Orange ‡, $p < 0.05$ relative to pWSK29.

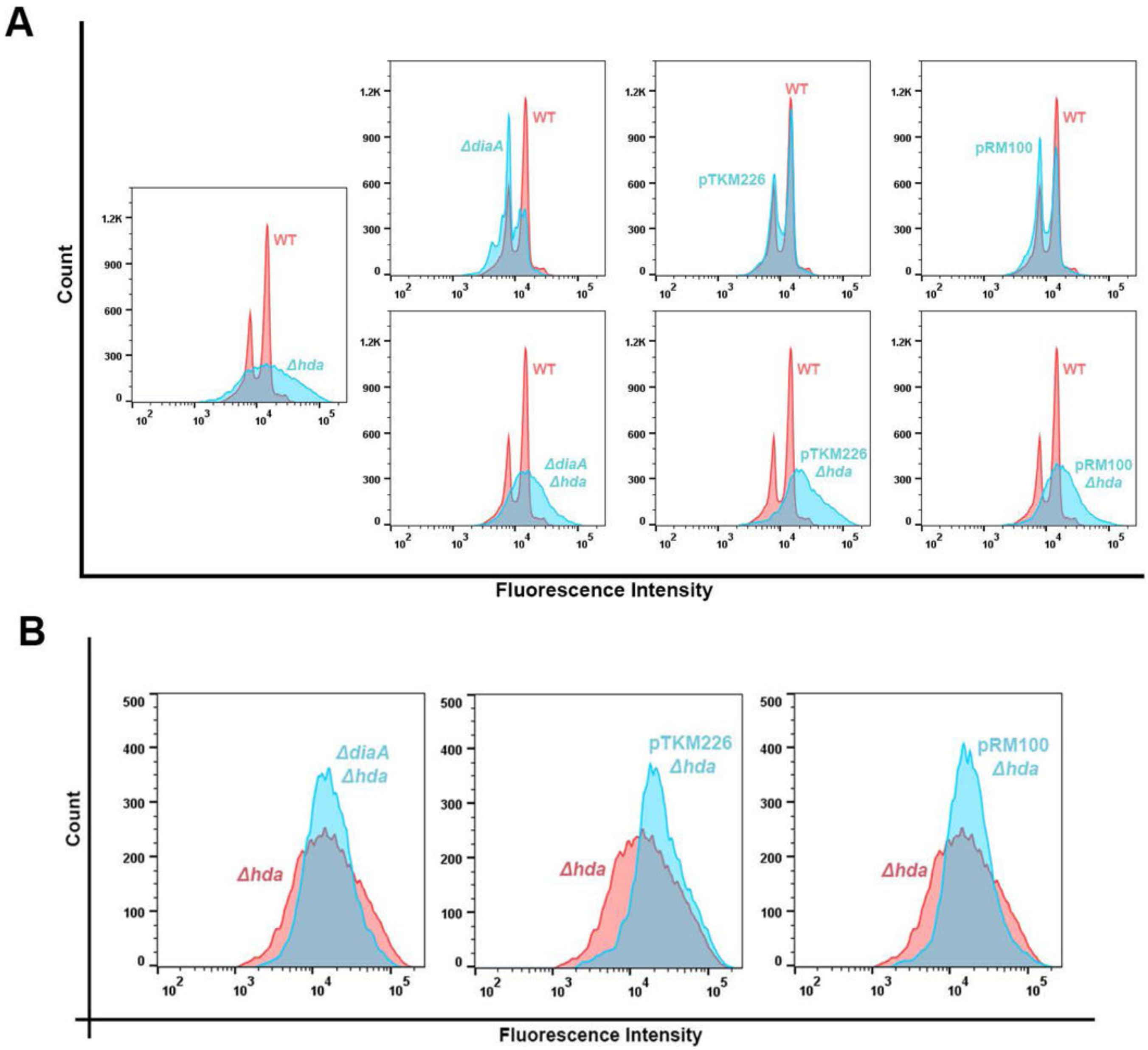

Figure 3. Cell cycle analysis of Δ*hda* suppressors

Genome content of the Δ*diaA* and pTKM226 or pRM100 bearing strains as a function of *hda* are shown as measured by flow cytometry. Respective profiles are overlaid on the **(A)** MG1655 wild type (hda^+) or **(B)** the isogenic Δ*hda* control. Results shown represent 20,000 events for each indicated strain. Fluorescence intensity (abscissa) is presented in logarithmic scale.

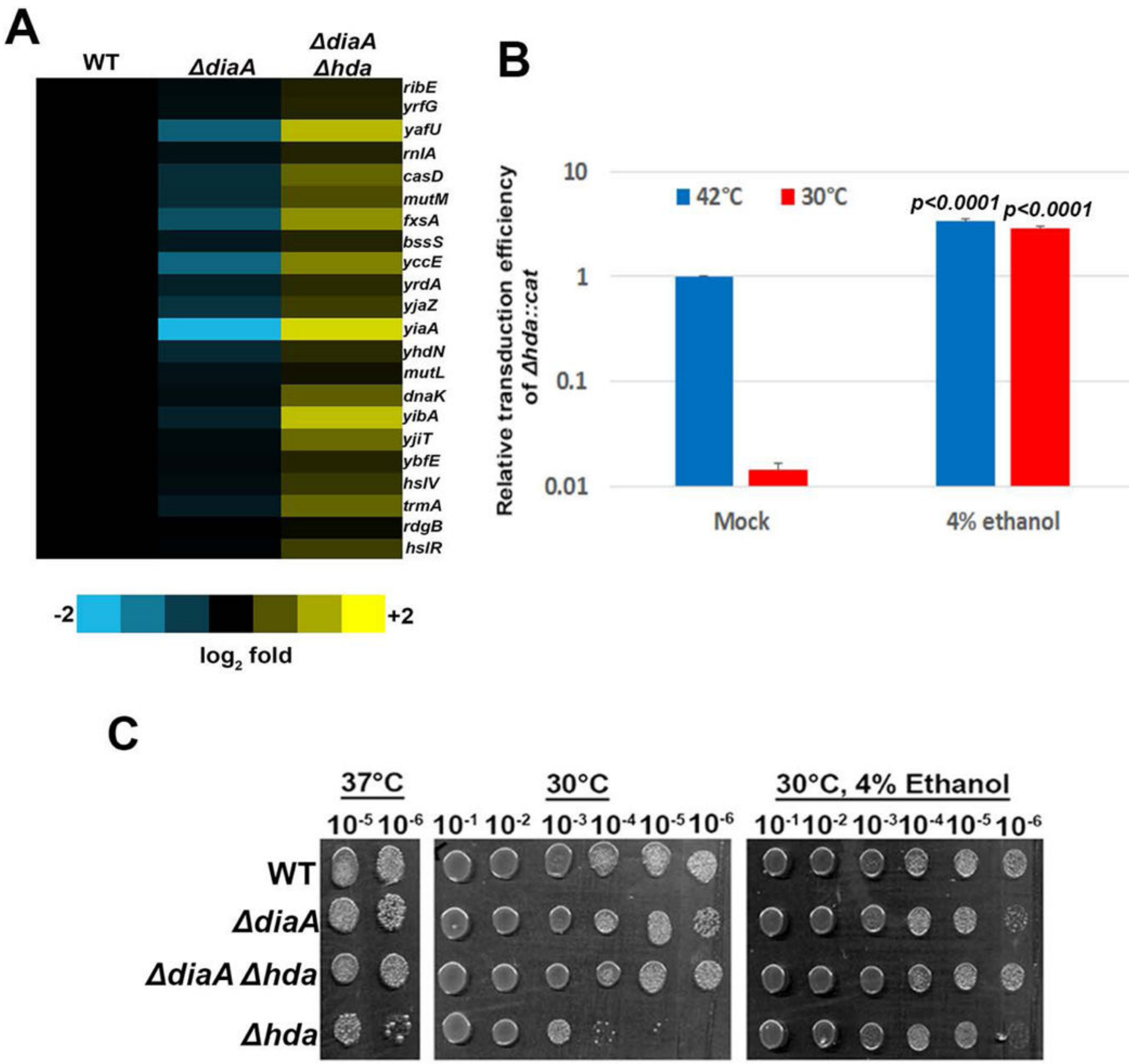

Figure 4. Induction of the heat shock response efficiently suppresses Δ*hda* cold sensitivity

(A) Respective expression levels of RpoH-regulated genes as measured by RNA-seq are represented in heat map form. **(B)** The ability of heat shock induction (addition of 4% ethanol) to suppress Δ*hda* cold sensitivity was measured using a quantitative Δ*hda*::*cat* P1*vir* transduction assay, **(C)** or a spotting assay, as described in Experimental Procedures. Results in panel B represent the average of 3 determinations ± one standard deviation. *P* values relative to the mock control are indicated (Student's t-test). Results in panel C are representative of 2 independent determinations.

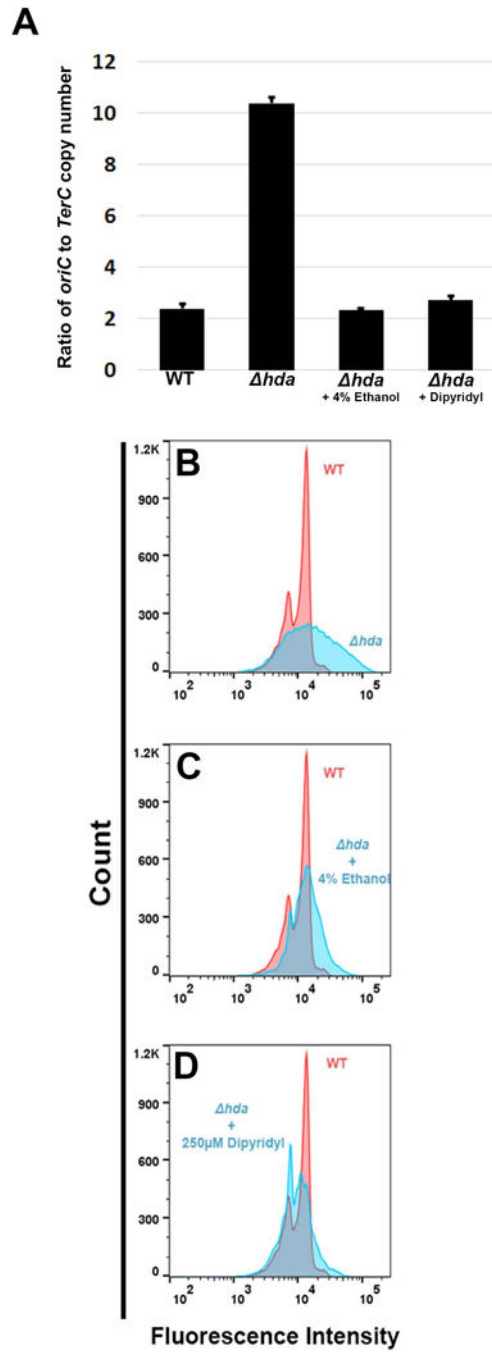

Figure 5. Effects of ethanol and dipyridyl on replication

(A) *oriC/terC* copy number ratios of MG1655 (WT) and JCB100u1 (Δ*hda*) with or without ethanol (4%) or dipyridyl (250 μM) were measured using qPCR, as described in Experimental Procedures. Flow cytometry was used to analyze genome content in **(B)** JBC100u1 (Δ*hda*), **(C)** JCB100u1 grown in the presence of 4% ethanol or **(D)** 250 μM dipyridyl, compared to MG1655. Flow cytometry data were collected for 20,000 events for each indicated strain. Fluorescence intensity (abscissa) is presented in logarithmic scale.

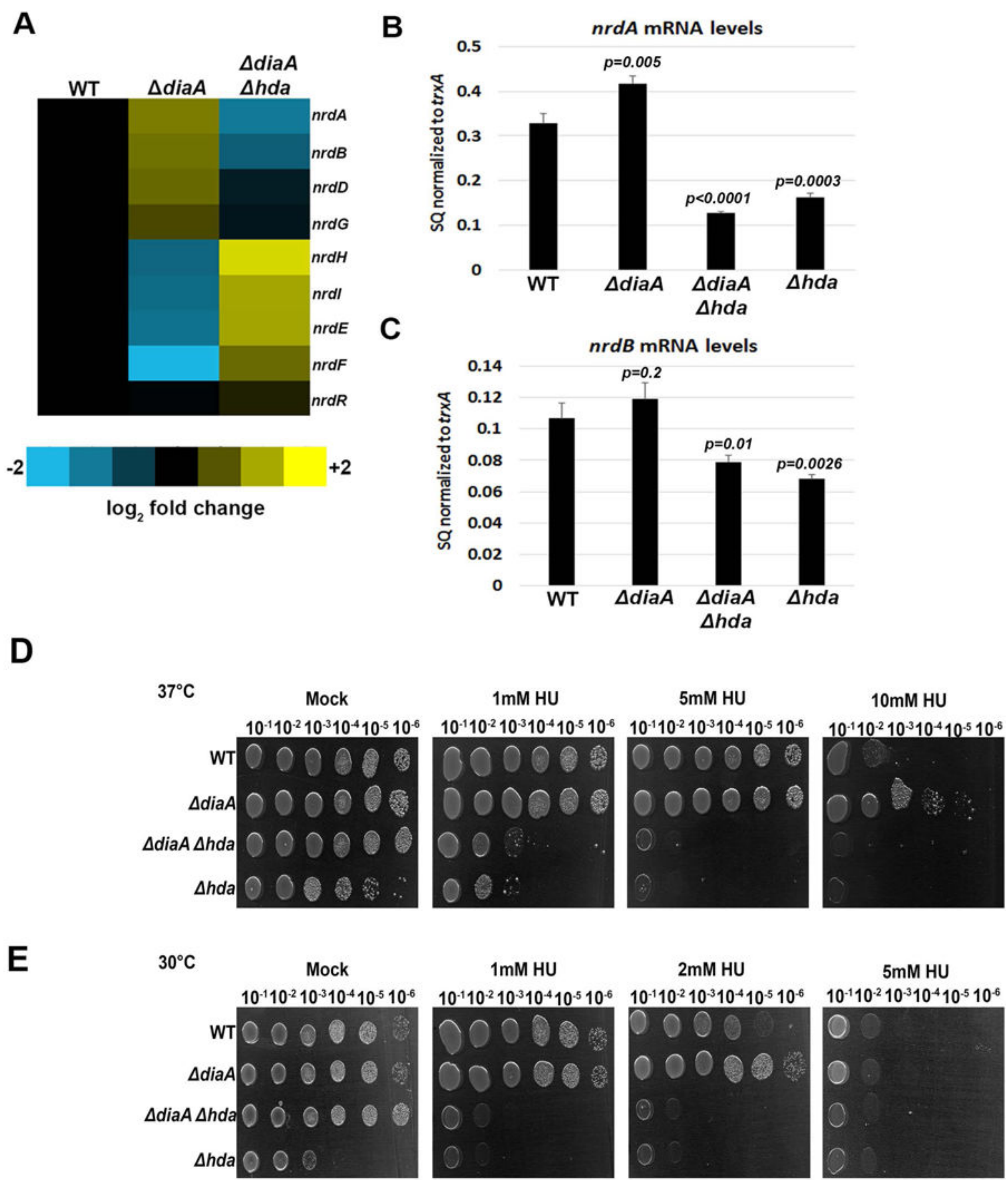

Figure 6. Effects of the Δ*diaA* and/or Δ*hda* alleles on *nrdAB* levels

(A) Respective expression levels of the different *nrd* genes as measured by RNA-seq are represented in heat map form. **(B)** Relative levels of *nrdA* and **(C)** *nrdB*, as measured by qPCR, are indicated. Results represent the average of 3 determinations ± one standard deviation. *P* values relative to the hda^{+} $diaA^{+}$ wild type (WT) control are indicated (Student's t-test). Relative sensitivities of the indicated strains to HU at **(D)** 37°C or **(E)** 30°C are indicated. Results shown in panels D and E are representative of 3 determinations.

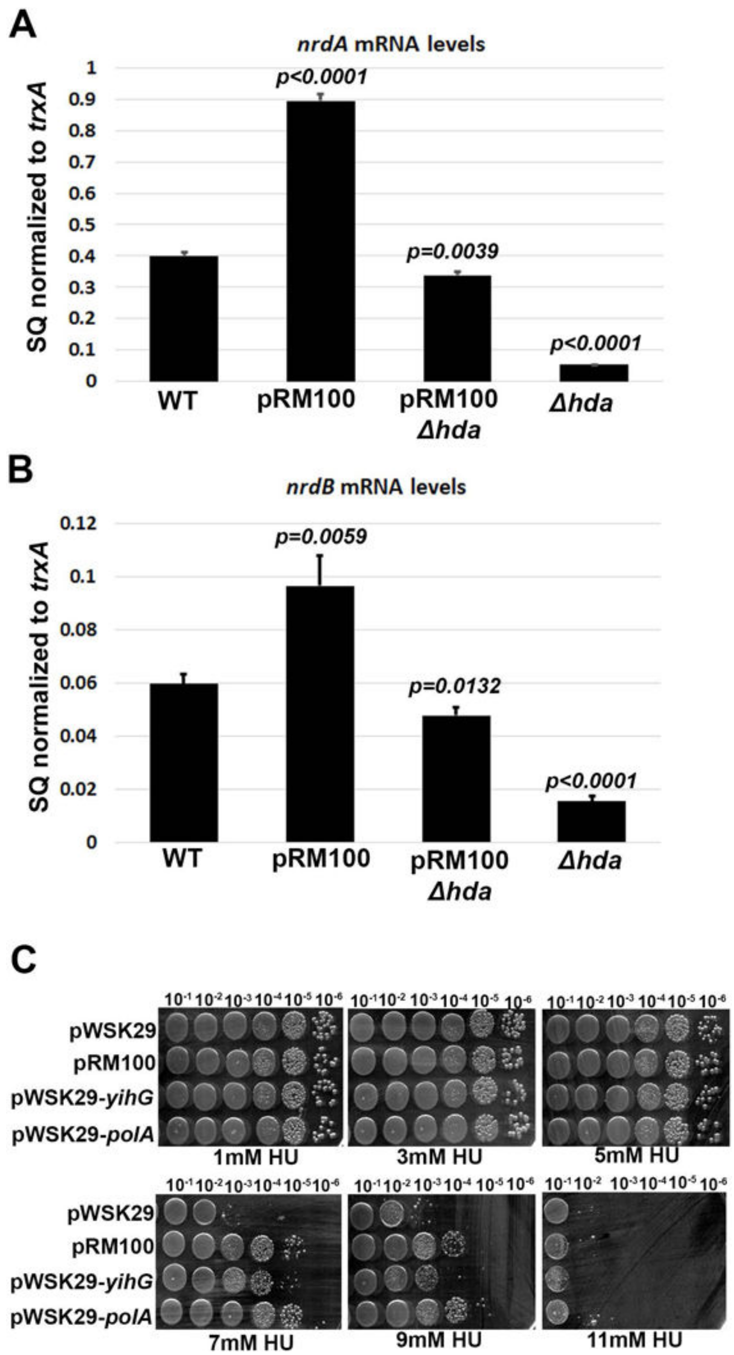

Figure 7. Overexpression of *yihG'–polA* acts to increase expression of *nrdAB*

(A) Relative levels of *nrdA* and **(B)** *nrdB*, as measured by qPCR, are indicated. Results represent the average of 3 determinations ± one standard deviation. *P* values relative to the *hda*$^+$ *diaA*$^+$ wild type (WT) control are indicated (Student's t-test). **(C)** Relative sensitivities of the indicated strains to HU at 37°C are indicated. Results shown are representative of 4 independent determinations.

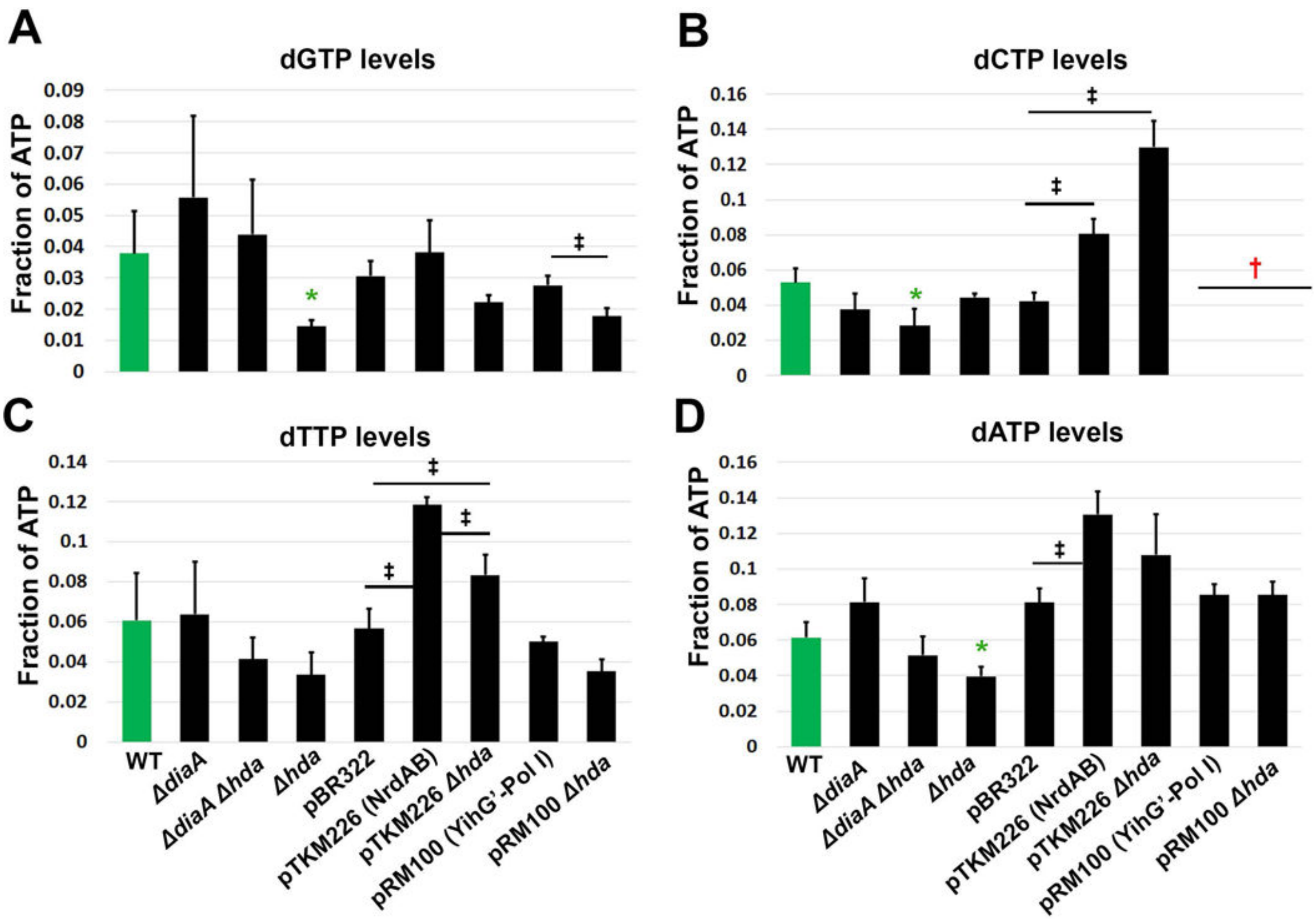

Figure 8. Relative dNTP levels in the different *sch* strains

Relative levels of each of the 4 dNTPs were measured in cultures grown at 37°C as described in Experimental Procedures. Strains are *hda*$^+$ unless otherwise stated. Results represent the average of 4 determinations ± one standard deviation. Symbols are as follows: ‡, compared values (black bar) are statistically significant $p < 0.05$; Green *, $p < 0.05$ relative to WT; Red †, the peak corresponding to dCTP was not sufficiently well resolved for reliable quantitation.

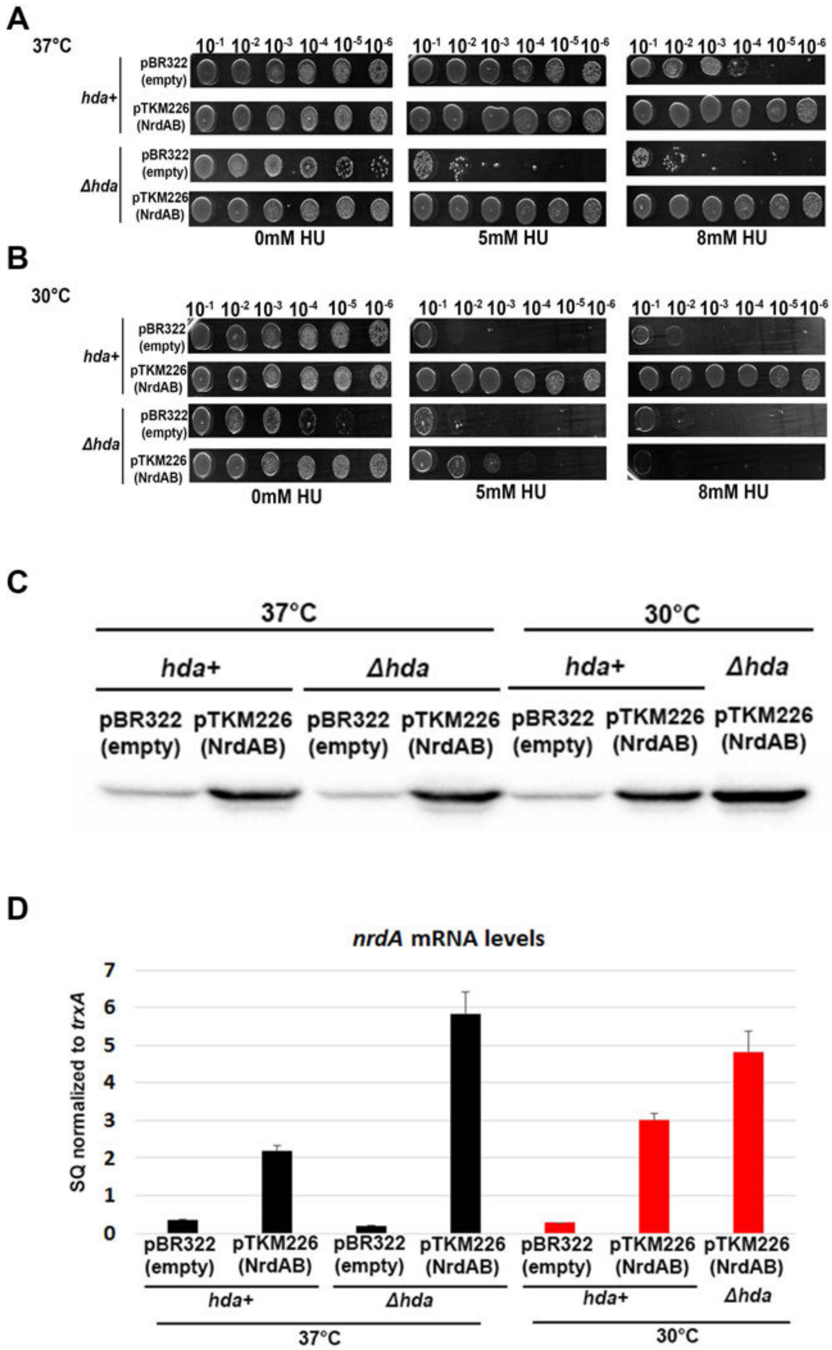

Figure 9. Loss of *hda* function sensitizes *E. coli* to HU at 30°C

(A & B) Respective sensitivities of isogenic *hda*$^+$ and Δ*hda* strains bearing either the pBR322 (control) or pTKM226 (NrdAB overexpressing) plasmid, as indicated, are shown. Results are representative of 2 determinations. **(C)** Western blot analysis of NrdB levels was performed as described in Experimental Procedures. Results are representative of 2 determinations. Average NrdB levels relative to the wild type (WT) control ± one standard deviation are shown. **(D)** Relative *nrdA* levels were measured using qPCR as described in

Experimental Procedures. Results represent an average of 3 determinations ± one standard deviation. *P* values are indicated (Student's t-test).

Author Manuscript
Author Manuscript
Author Manuscript

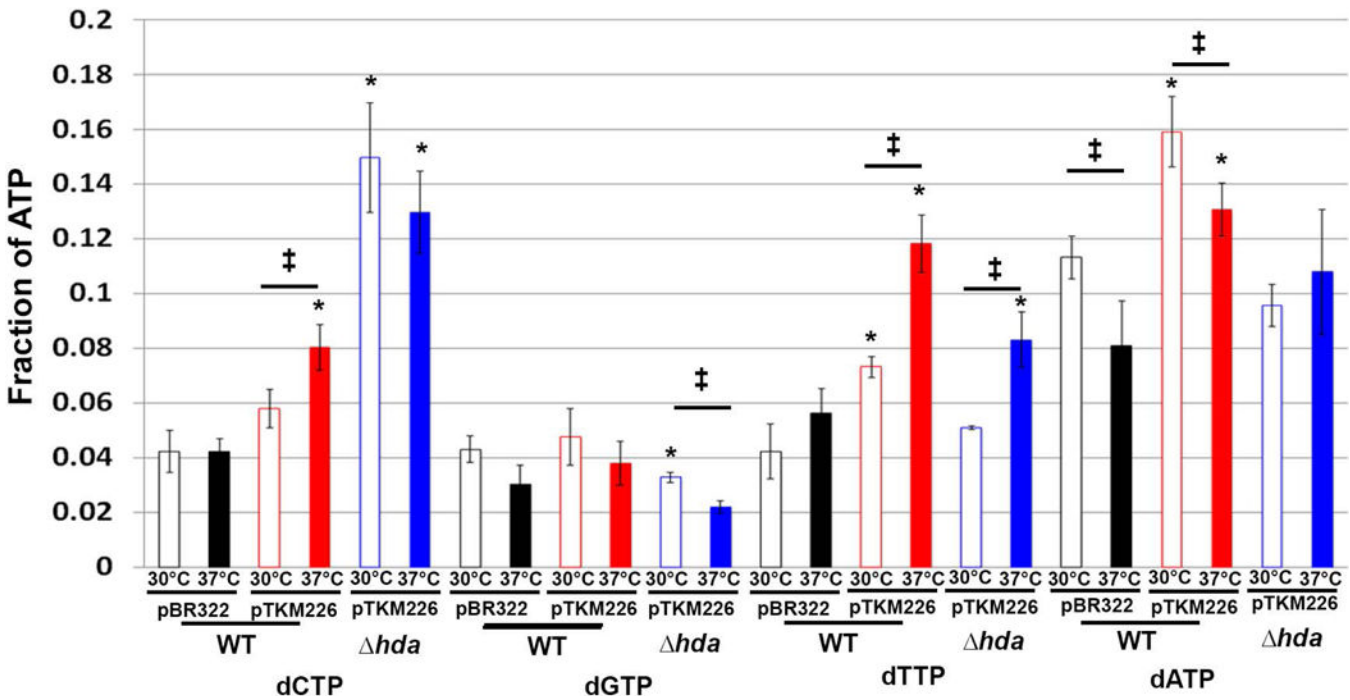

Figure 10. Respective levels of dNTPs in strains grown at 30° or 37°C

Levels of each of the 4 dNTPs present in the indicated *hda*+ and Δ*hda* strains bearing either the pBR322 (control) or pTKM226 (NrdAB overexpressing) plasmid were measured as described in Experimental Procedures. Cultures were grown at 30° or 37°C, as indicated. Results represent the average of 4 determinations ± one standard deviation. Symbols are as follows: ‡, $p < 0.05$ as indicated by the black bar; *, $p < 0.05$ relative to pBR322 at respective temperatures.

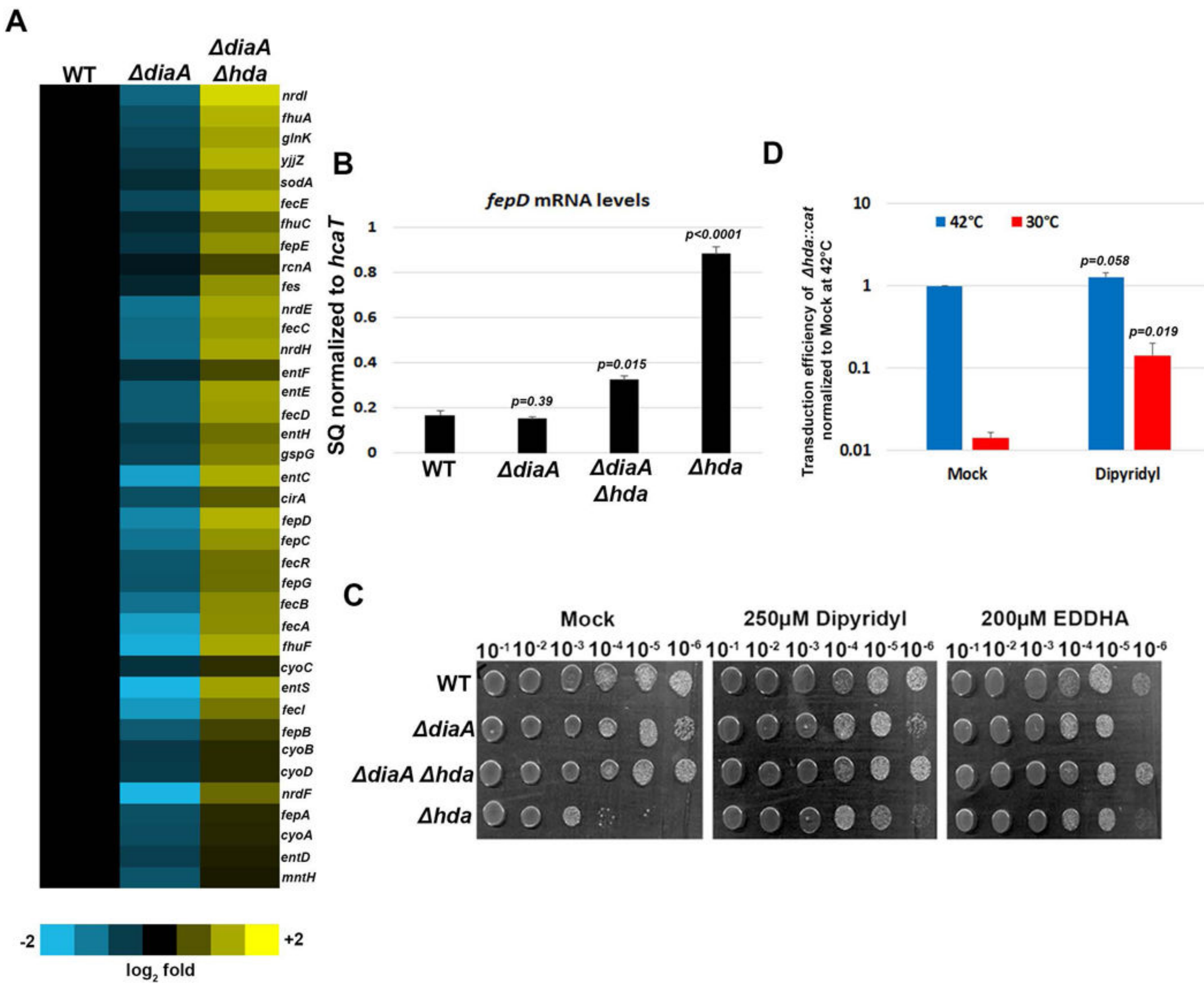

Figure 11. The Fur regulon is derepressed in the Δ*hda* strain

(A) Expression levels of the respective Fur-regulated genes as measured by RNA-seq are represented in heat map form. **(B)** Relative levels of *fepD*, as measured by qPCR, are indicated. Results represent the average of 3 determinations ± one standard deviation. *P* values relative to the hda^+ $diaA^+$ wild type (WT) control are indicated (Student's t-test). **(C)** The ability of the iron chelators dipyridyl or EDDHA to suppress Δ*hda* cold sensitivity at 30°C in a spotting assays is shown. These results are representative of 2 determinations. **(D)** The ability of dipyridyl to suppress Δ*hda* cold sensitivity as measured by a quantitative P1*vir* transduction assay is shown. Results represent the average of 3 determinations ± one standard deviation. *P* values are indicated (Student's t-test).

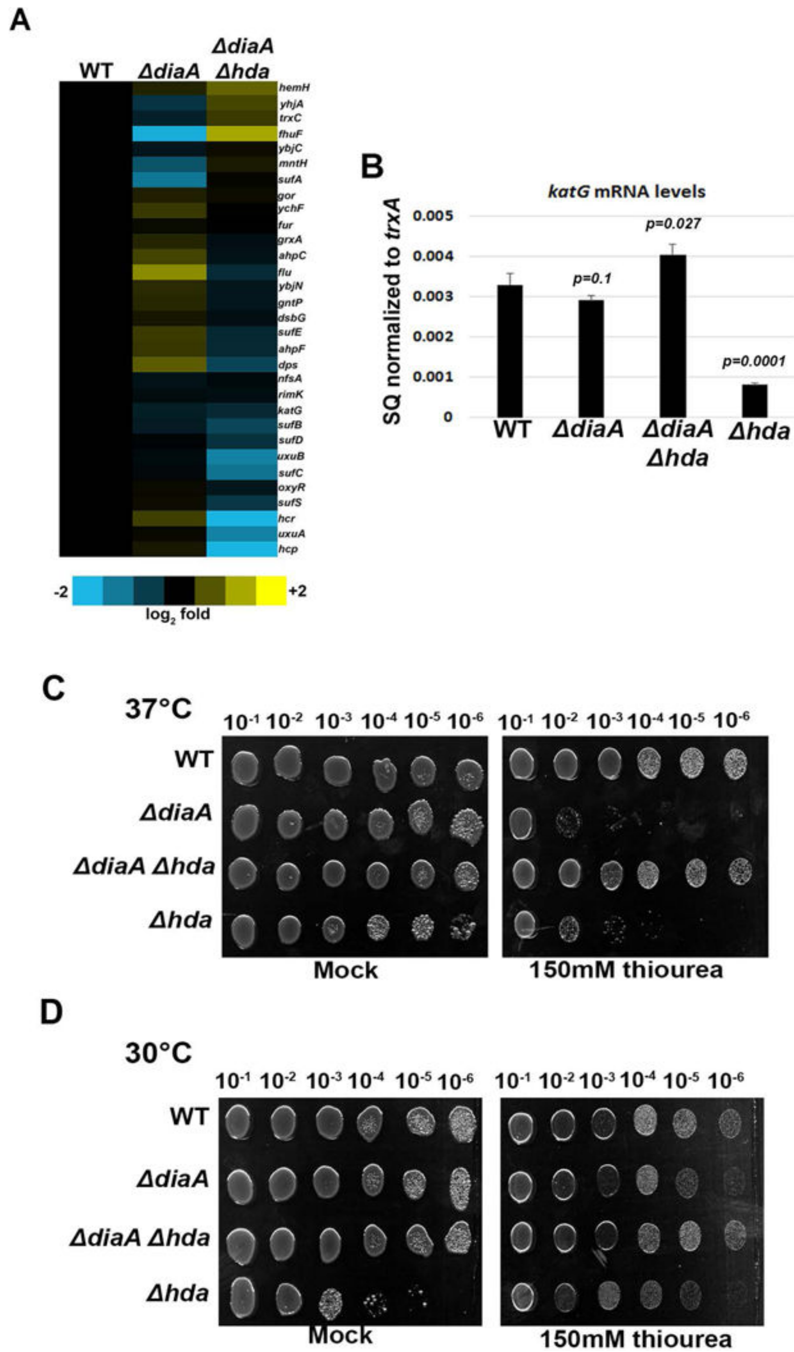

Figure 12. The OxyR regulon is repressed in the Δhda strain

(A) Expression levels of the respective OxyR-regulated genes as measured by RNA-seq are represented in heat map form. **(B)** Relative levels of *katG*, as measured by qPCR, are indicated. Results represent the average of 3 determinations ± one standard deviation. *P* values relative to the hda^{+} $diaA^{+}$ wild type (WT) control are indicated (Student's t-test). **(C & D)** The ability of thiourea to suppress Δ*hda* cold sensitivity was measured as described in Experimental Procedures.

Table 1

Summary of sequence analysis of suppressors of Δ*hda* cold sensitivity.

Strain	***sch* allele**	**Suppressor(s)**
JCB100s1	*sch*-1	IS5 insertion upstream of *nrdA* coding sequence
JCB100s2	*sch*-2	IS5 insertion within the *diaA* coding sequence
JCB100s4	*sch*-4	IS5 insertion upstream of *nrdA*
JCB100s6	*sch*-6	IS5 insertion upstream of *nrdA*
JCB100s7	*sch*-7	IS5 insertion upstream of *nrdA*
JCB100s8	*sch*-8	IS1 insertion upstream of *nrdA*
JCB100s9	*sch*-9	IS5 insertion upstream of *nrdA*
JCB100s10	*sch*-10	Duplication of the 180-kb region between *rrsA* and *rrsE* (86.95 min–90.67 min)
		G142A point mutation (Ala-48-Thr) in *trmA* (TrmA-A48T)
JCB100s12	*sch*-12	Duplication of the 180-kb region between *rrsA* and *rrsE* (86.95 min–90.67 min)